MASTER

MATHEMATICAL FINANCE

MASTER'S FINAL WORK

REPORT

MODELS FOR SPREAD OPTION PRICING IN ENERGY MARKETS

FILIPE FELICIANO DINIS TOMÉ

OCTOBER - 2024

Lisbon School of Economics & Management
Universidade de Lisboa

MASTER

MATHEMATICAL FINANCE

MASTER'S FINAL WORK

REPORT

MODELS FOR SPREAD OPTION PRICING IN ENERGY MARKETS

FILIPE FELICIANO DINIS TOMÉ

SUPERVISION:

PROF. JOÃO MIGUEL GUERRA

DR. RODRIGO BRAAMCAMP

OCTOBER - 2024

Dedicated to my mother.

ABSTRACT

The European energy landscape is undergoing a significant transformation, driven by the increasing importance of electrical interconnections.

Interconnectors, which are high-voltage cables linking neighboring electricity systems, facilitate efficient power exchange across regions, balancing supply and demand while leveraging renewable resources. They help harmonize energy prices, promoting economic welfare, but technical constraints can lead to congestion and price disparities, resulting in inefficiencies.

To manage price fluctuations arising from these challenges, financial derivatives, particularly spread options, are employed. This work discusses two models for pricing spread options based on the interconnected electricity markets of Spain and France. The first model utilizes Margrabe's formula, while the second is designed to model the spread between power spot prices through mean-reverting processes. Subsequently, option prices are computed based on the prices generated from this spread model. A new approach refines this second model by incorporating the price difference between power futures as an input.

Additionally, a trading strategy based on this new approach is developed, aiming to capitalize on auction pricing inefficiencies.

The findings indicate that, despite the inherent risks involved in trading transmission rights due to the volatility and uncertainty in the electricity market, the model's results still provide valuable insights that assist traders in making informed bidding decisions during auctions for these rights.

KEYWORDS: Interconnectors; Congestion; Volatility; Spread Options; Jumps; Transmission Rights.

JEL CODES: C51; D44; G13; Q41.

TABLE OF CONTENTS

Abstract i

Table of Contents ii

List of Figures iv

List of Tables v

Acknowledgements vi

1 Introduction 1

2 Theoretical Foundations 3

2.1 What are interconnectors and their economy 3
2.2 European Day-ahead Market 4
2.3 Congestion Risk 5
2.4 Physical Transmission Rights (PTRs) 6
2.5 Financial Transmission Rights (FTRs) 6
2.6 Remuneration of PTRs with 'UIOSI' and FTRs 7
2.7 Auctions for FTR Options 8
2.8 How do FTR options work 9

3 Spread Option Tool 10

3.1 Margrabe's Model 11
3.2 Model Assumptions and Close Form Solution 11
3.3 FTR option tool implementation with Margrabe formula 13

4 Stochastic Model for Spread Option 14

4.1 Literature Review 14
4.2 Data Information 16
4.3 Spread Option Modelling 18
4.4 Option Valuation 19
4.5 Implementation of The Spread Price Modelling 20
4.6 Compound Poisson process parameters 27
4.7 Backtesting 28

5 New Methodology 30

5.1 Backtesting of the new methodology 32

6 Conclusions **35**

References **36**

A Fundamental concepts about Interconnection Auctions **38**
A.1 Market Time Unit (MTU) 38
A.2 Transmission System Operator (TSO) 38
A.3 Single Allocation Platform 38
A.4 Power Exchange 38

B Stochastic Processes **39**
B.1 Stochastic Process 39

C Time-Series **42**
C.1 Error Measures 42

D Statistical Tests **43**
D.1 Kolmogorov-Smirnov Test 43

E Simulations **43**
E.1 Price Process Simulation Model 1 43
E.2 Price Process Simulation Model 2 45

F Additional Data **46**

LIST OF FIGURES

1 Congestion. Reprinted from Gautier (2019) 3
2 Spread Option Payoffs 9
3 Historical hourly spread price for the interconnection FR $\rightarrow$ SP in Euros . 17
4 Price differentials "Spain minus France" with day ahead prices (2010-2020) 20
5 Seasonality function for Spain/France 22
6 ACF and PACF of the detrended and deseasonalized time-series 22
7 ACF and PACF of the adjusted AR(1) model 23
8 Histogram of the AR(1) residuals limited between -100 and 100 (left) and corresponding QQ-plot for normality (right). 24
9 Identification of normal variations using the recursive filtering procedure . 26
10 Identification of normal variations using the recursive filtering procedure . 26
11 Histogram of positive and negative jumps with the fitted shifted exponential distribution 28
12 Comparison between Realized Premium and Predicted Option Premiums for interconnection FR $\rightarrow$ SP 29
13 Comparison between Realized Premium and Predicted Option Premiums for interconnection SP $\rightarrow$ FR 30
14 Comparison between Realized Premium and Predicted Option Premiums for interconnection FR $\rightarrow$ SP 33
15 Comparison between Realized Premium and Predicted Option Premiums for interconnection SP $\rightarrow$ FR 33
18 Hourly spread zero during January 2019 46

List of Tables

I Coefficients Spain/France 21

II Jump identification and removal - recursive filtering procedure. 25

III Results and Data Summary. * Indicates instances where the auction was not executed. 32

IV Results of Trading Strategy. * Highlight the cases in which the auction failed to occur. 34

Acknowledgements

I would like to thank Professor João Guerra for his guidance.

I am also grateful to my friends, Nádia Ilhéu and Rodrigo Martins, for their support and helpful discussions.

Finally, I want to express my appreciation to my parents for their unwavering support and encouragement throughout this journey.

1 Introduction

The European energy landscape is currently undergoing a significant transformation, marked by the increasing importance of electrical interconnections. Interconnectors, high-voltage cables that link the electricity systems of neighboring countries, play a crucial role in facilitating cross-border power exchange. These infrastructures help bridge the gap between supply and demand in European electricity markets by enabling the transmission of electricity across different locations.

In Europe, these locations are delimited by the various Transmission System Operators (TSOs) and can represent either a country or a larger bidding zone. For example, France is interconnected with Belgium, Switzerland, Germany, Spain, and Italy. Additionally, Spain connects with Portugal and France, while Portugal has a connection with Spain.

This interconnection market is managed by the European Network of Transmission System Operators for Electricity (ENTSO-E), working with European Transmission System Operators to ensure the security of the interconnected power grid across all time frames and to support the efficient operation and development of Europe's electricity markets.

Interconnectors play a vital role in exploiting price differences through power imports and exports. By facilitating the flow of electricity across borders, they drive price alignment between countries, promoting economic and social welfare. However, technical constraints sometimes prevent the full transmission of power across countries, leading to price differentials between zones. This creates congestion costs, which represent the additional expenses incurred from relying on more expensive electricity sources in areas with high demand.

To address the price fluctuations arising from grid congestion and the associated congestion costs, market participants need effective mechanisms to hedge against these risks. Financial derivatives, particularly spread options, play a crucial role in this context by allowing participants to manage their exposure to price differences between locations.

A spread option is a type of option contract that derives its value from the difference, or spread, between the prices of two or more assets.

In the context of energy markets, spread options are extensively used, particularly concerning the interconnection between market zones. TSOs issue these options through auctions managed by specialized entities. This allows all market participants seeking to purchase these derivatives to access an auction platform where they can trade transmission capacity rights to mitigate their risk. For instance, when a participant buys an option in the Spain $\rightarrow$ France interconnection, he buys the right to transmit energy for each hour of the period considered from Spain to France, and, if the flux is financial, the payoff of such option is the hourly spread between France and Spain power spot price, in case it is positive.

Although spread options are mainly used by suppliers in energy markets as hedging tools, they can also serve as speculative instruments for commodity trading firms.

This work proposes a valuation tool that employs real options theory to assess the pricing of interconnection options, utilizing market data for the interconnected markets of Spain and France. The value of an interconnection option is represented as a bundle of European-style options based on the spread between the two markets, with the valuation formula derived through Monte Carlo simulations. The model developed for the spread accounts for price jumps in both directions, incorporates volatility, and includes mean reversion to a seasonal trend. Additionally, a novel methodology has been implemented, which integrates the futures locational spread between the two markets, providing a forward-looking perspective to the model.

Following this, the profit and loss (P&L) from a trading strategy, which is the primary goal of this work, is presented. This strategy involves placing bids for transmission rights on the auction platform and is based on model-derived prices, aiming to capitalize on potential underpricing of the auction's marginal price.

This Master's Final Work represents the culmination of an internship at Energias De Portugal (EDP) within the Trading Modelling department. The project is organized into three main parts, following a structured schedule designed to systematically explore and develop key concepts and models to energy markets, with a particular emphasis on interconnection options.

First, the initial task was to prepare a document outlining the primary concepts behind the interconnection market, leading to the corresponding chapter *Theoretical Foundations*.

Building on this theoretical groundwork, the next phase of the internship involved developing a tool for spread options in the context of energy markets, using Python. This tool primarily utilized Margrabe's formula, a well-established framework for pricing spread options. The development and application of this tool are detailed in the chapter *Spread Option Tool*.

The third and final phase of the internship focused on constructing the model for spread options within the context of cross-border electricity trading, specifically addressing the limitations of Margrabe's formula in this domain, aimed to implement the trading strategy. This model-building process and its results are thoroughly explained in the chapter *Stochastic Model for Spread Option*. Furthermore, the new methodology, its results, and the P&L from the trading strategy, are presented in the chapter *New Methodology*.

2 THEORETICAL FOUNDATIONS

This section offers an overview of the interconnection market, which corresponds to the first task of the internship focused on developing a document that outlines the key concepts essential to modern energy markets.

2.1 What are interconnectors and their economy

Interconnectors enable cross-border energy flows between two markets, helping balance supply and demand. Consider two zones: Zone S, which has higher electricity demand than supply, and Zone N, which has more supply than demand. When interconnector capacity is sufficient, excess demand in Zone S can be met by electricity flowing from Zone N, leading to price convergence. In this scenario, the lowest-cost producer sets the market price for both Zones.

However, if the interconnector capacity is exceeded, congestion occurs. This happens when the transmission network is overloaded, restricting the flow of lower-priced electricity from Zone N to Zone S. Although electricity continues to flow through the interconnector, the limited capacity prevents the full transfer of cheaper electricity. As a result, consumers in Zone S face higher electricity prices, while consumers in Zone N face lower prices.

Axel Gautier illustrated this situation in Figure 1.

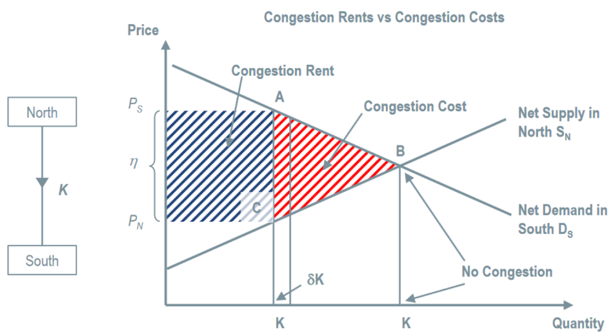

FIGURE 1: Congestion. Reprinted from Gautier (2019)

The figure represents the net supply in Zone N and the net demand in Zone S. Electricity should flow from N to S and in the absence of congestion, prices should converge (point B on the figure) with the lowest-cost producer setting the market price for both Zones. There is, however, a physical limit to cross-border trade given by the capacity of the interconnecting lines, denoted by K.

According to Gautier, if the electricity required to converge prices surpasses the grid's capacity, the line becomes congested, causing prices to diverge. Conversely, if the power flow needed for price convergence is within the interconnection capacity, the line remains uncongested. In Figure 1, the inability to transmit sufficient cheaper electricity from Zone N to Zone S creates a surplus of supply in Zone N. This surplus leads to downward pressure on prices, resulting in lower market prices in Zone N. Meanwhile, buyers in Zone S face higher prices because they cannot access enough of the more affordable electricity from Zone N to meet their demand.

2.2 European Day-ahead Market

The market value of energy commodities is fundamentally tied to their delivery date and location. Unlike gas and oil, which can be stored or have their delivery postponed, electricity must be consumed immediately due to its inherent inability to be stored. As a result, electricity is primarily traded in the day-ahead market, where prices are established one day in advance through an auction mechanism.

In most European countries, day-ahead spot prices are determined using a common price coupling algorithm known as PCR Euphemia. Each day at 12:00 CET (Central European Time), an auction is held to set electricity prices and capacities for the following day. During this auction, market participants submit bids to sell electricity and offers to buy electricity for each of the next 24 hours. Sellers specify the quantity of electricity they wish to sell and at what price, while buyers indicate how much electricity they want to purchase and at what price. The resulting prices are influenced by the principles of supply and demand, as discussed in 2.1.

The Euphemia algorithm optimizes the allocation of available interconnector capacity through a process known as market coupling. Before market coupling was introduced, trading members had to first reserve cross-border capacity and then engage in separate transactions to purchase electricity, which was inefficient.

With market coupling, these processes are integrated into a single mechanism. Participants submit their bids and offers for electricity, and the algorithm simultaneously considers the available transmission capacity between zones to determine the optimal flow of electricity and the resulting spot prices. This approach maximizes welfare across interconnected regions while effectively balancing supply and demand across borders.

The Euphemia algorithm is utilized across numerous European countries, including Spain, Portugal, Germany, France, Italy, and the Nordics. Its efficiency is evident in the increasing price convergence observed between these market areas. When the interconnection lines between two countries are not saturated, prices align, resulting in a zero spread, indicating a coupled market. Conversely, when capacity is insufficient and prices differ, the market is considered decoupled.

Figure 18 in Appendix illustrates how often the hourly spread for the interconnection from France to Spain was zero during January 2019.

2.3 Congestion Risk

For suppliers contracted to deliver electricity from Zone N to buyers in Zone S, congestion introduces significant financial risks. This is because congestion can prevent them from transporting enough electricity to fully meet their contractual obligations. As a result, they may need to purchase additional power in Zone S at higher prices, further increasing their costs.

For example, if a supplier in Zone N has a contract to deliver electricity to Zone S at €30/MW during a specific hour, but the price in Zone S rises to €50/MW due to congestion, the supplier faces a €20/MW loss for each megawatt he cannot transmit. This loss occurs because he must buy electricity at the higher price in Zone S to meet his contractual obligations while receiving only the lower price in Zone N. The financial impact of the €20/MW price differential can significantly reduce profitability or turn a profitable contract into a loss.

To manage these risks, suppliers often turn to the transmission rights market, a secondary market which offers mechanisms for hedging against price differentials. In this market, participants can buy and sell Long-Term Transmission Rights (LTTRs), which grant them the ability to transmit a specified amount of electricity across a interconnector for a designated period. If the transmission is physical, LTTRs give suppliers guaranteed access to the grid at a predictable cost, allowing them to avoid financial losses that can arise during peak demand periods and ensure they can deliver a portion or the full amount of contracted energy. If the transmission is financial, LTTRs act as hedging instruments that allow market participants to benefit from the price difference between two zones. In this case, rather than physically delivering electricity, the holder of the LTTR receives a payout based on the price differential between the zones, helping to offset losses from price volatility.

European Union law requires TSOs to issue LTTRs. TSOs facilitate access to these rights through auction-based mechanisms, allowing market participants to bid for the capacity needed to transmit electricity. LTTRs are categorized into Physical Transmission Rights and Financial Transmission Rights.

2.4 Physical Transmission Rights (PTRs)

According to Article 2 of the *Harmonised Allocation Rules for Long-Term Transmission Rights* Agency for the Cooperation of Energy Regulators (ACER) (2023), Physical Transmission Rights (PTRs) are entitlements that grant the holder the exclusive right to use a specific interconnection in one direction to transfer a predetermined quantity of energy from one market hub to another, over a designated period.

PTRs serve as a hedging instrument because they allow market participants to secure predictable access to transmission capacity at a fixed price determined by the primary auction mechanism. This provides predictable costs for accessing the interconnector and guarantees access to the grid to meet contractual obligations.

Since the holder has secured and nominated the physical transfer of electricity, there is no need to participate in the day-ahead market for this portion of his supply.

PTRs can also be allocated under the 'Use-It-Or-Sell-It' (UIOSI) principle, allowing the holder to receive market spread remuneration for each megawatt (MW) of PTRs he holds if he chooses not to use the physical capacity, provided the spread is positive.

Furthermore, Article 45 of the same document specifies that if the holder does not nominate his PTR for physical use, the underlying capacity of this non-nominated PTR gets resold in the day-ahead market.

In this scenario, for the portion of the transmission rights that the holder did not nominate for physical use, he must engage in the day-ahead market. He will act as a buyer in the destination area while selling at the price of the supplying area. This ensures he can meet his energy supply contract in the destination area for the rights he chose not to nominate, receiving market spread remuneration for that unused capacity in case there is congestion in the grid.

2.5 Financial Transmission Rights (FTRs)

In contrast, Financial Transmission Rights (FTRs) are purely financial instruments. As outlined in Article 2 of *Harmonised Allocation Rules for Long-Term Transmission Rights* Agency for the Cooperation of Energy Regulators (ACER) (2023), FTRs entitle the holder to receive the market spread between two market hubs, provided it is positive, for each MW of FTRs held, during a designated period. An FTR option from Market A to Market B allows the holder to hedge price differences between market zones by receiving compensation when the spread is positive, at a cost determined by the FTR auction mechanism.

Unlike PTRs, FTRs do not provide physical access to the electricity grid or the right to nominate electricity flows. They are exclusively used for financial hedging purposes. In this case, the supplier must participate in both markets to ensure the supply of energy.

For instance, consider the scenario described in Section 2.1, where a supplier in market N has a supply contract set at €30/MW for a specific hour. Due to congestion, he cannot fully meet his contractual obligations in market S, where prices have risen to €50/MW. As a result, to fulfill the contract, he must purchase electricity at the higher price in market S for that hour. This leads to a loss of €20/MW for every megawatt he is unable to transmit, as he is purchasing at €50/MW but selling at only €30/MW. However, by holding the FTR, the supplier receives a payout of €20/MW, compensating for the price difference between the two markets during that specific hour. The same principle applies to non-nominated PTRs under the 'UIOSI' mechanism, which are resold in the day-ahead market. Since both FTRs and non-nominated PTRs represent financial, not physical, rights, the associated transmission capacity remains under the control of TSOs and Power Exchanges (PXs). These entities utilize this capacity by selling it in the day-ahead market for energy trading between market hubs. The revenue generated from these sales, driven by the price spread between market areas, is then used to fulfill the payouts to FTR and non-nominated PTR holders.

Both non-nominated PTRs with the 'UIOSI' option and FTRs offer equivalent financial hedging capabilities, providing the same level of risk management related to price differences between market hubs. It is important to note that if the market spread between the two hubs is negative, no financial compensation is provided to the non-nominated PTR with 'UIOSI' or FTR holders.

FTRs and non-nominated PTRs are attractive not only for hedging risks in cross-zonal energy transfers but also for their potential to enhance profits in trading activities.

2.6 Remuneration of PTRs with 'UIOSI' and FTRs

According to Article 48 of the *Harmonised Allocation Rules for Long-Term Transmission Rights* Agency for the Cooperation of Energy Regulators (ACER) (2023), for PTRs under the 'Use-It-Or-Sell-It' (UIOSI) principle, the single allocation platform compensates the holder for each megawatt (MW) per market time unit (MTU) that is not nominated. Typically, MTU corresponds to one hour, so this compensation is calculated per-megawatt for each hour that is not nominated.

The remuneration is determined based on the difference between the capacity to which the holder was entitled and what he actually used, multiplied by the positive price differential between the two spot markets specified, for each hour in the designated period.

Similarly, the document specifies that for FTRs, the holder is compensated for the full capacity he owns, regardless of usage. The remuneration is based on the agreed volumes, multiplied by the positive price differential between the two spot markets specified, for each hour in the designated period.

In the specific context of the interconnection between Spain and France, which will be the focus of this work, compensation is calculated per MW per hour, a measurement referred to as 'MWh' in energy markets.

2.7 Auctions for FTR Options

In the context of energy markets, auctions are classified into implicit and explicit types, each serving distinct purposes and timeframes.

Implicit auctions are the mechanism used in the European day-ahead market, where market participants submit bids and offers specifying the price and quantity of electricity they are willing to trade. This process facilitates the efficient allocation of transmission capacity alongside electricity trading.

In contrast, explicit auction is when the transmission capacity on an interconnector is auctioned to the market separately and independently from the marketplaces where electrical energy is auctioned. These auctions are dedicated to long-term capacity allocation, allowing market participants to secure transmission rights over extended periods, such as monthly or yearly.

The Joint Allocation Office (JAO) serves as the single allocation platform that administers FTR options to registered participants through an explicit auction process.

Each registered participant fulfilling the requirements for participating in the FTR auction may place bids in the auction tool until the relevant deadline for placing bids, according to the respective auction specification. Each bid specifies the amount of capacity the participant wishes to transmit and the price he is willing to pay.

The allocation of FTR options is structured around various standard timeframes. Commonly, they are offered in yearly timeframes, covering the entire calendar year from January 1 to December 31, and monthly timeframes, spanning from the first to the last day of each calendar month. Depending on the specific market design, these options can also be available in additional timeframes, including quarterly (three-month periods), seasonal, weekly and daily.

Once the bidding period concludes, the single allocation platform determines the auction results and allocates the FTR options.

Furthermore, the determination of auction results includes setting the marginal price for the bidding border and the amount of MW that each winner can transmit. This marginal price represents the cost per MWh for the right to transmit electricity in a specific direction. It is considered a sunk cost, as it must be paid regardless of whether there is a positive market spread from the congestion during the usage period.

2.8 How do FTR options work

Given the characteristics of FTR options, these are commonly called spread options, corresponding to an option written on the spread between two spot markets. Lion Hirth, Ingmar Schlecht and Anselm Eicke explain in Hirth et al. (2024) that a spread option, specifically a call option for the interconnection A $\rightarrow$ B, results in a payout from the option writer (TSO) to the option holder (the buyer) if the hourly spot price spread ("B minus A") is positive. Conversely, if the spread is negative, there is no payout. The reverse option, for the interconnection B $\rightarrow$ A, also known as a put option A $\rightarrow$ B, results in a payout from the writer to the holder if the spread is negative. Therefore, when a pair of options is issued, there is always a settlement payment from the TSO to the buyer. However, if the spread is zero, there is no payment from either side. Figure 2 below shows the payoff of the pair of options.

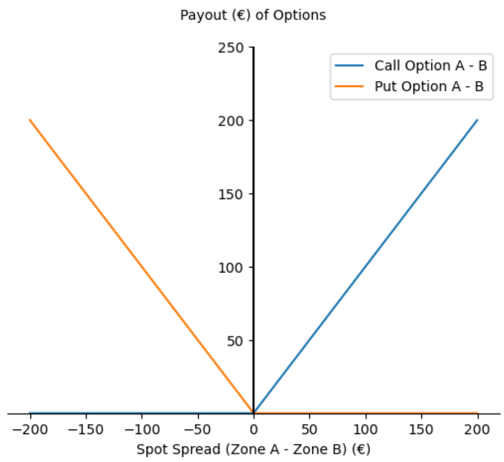

FIGURE 2: Spread Option Payoffs

The primary question is whether the congestion income, within the specified time frame of the transmission rights, is sufficient to cover the total auction sunk costs for acquiring these rights.

For example, consider a monthly FTR option with an auction marginal price of €7.25 per MWh. If the average price spread for that month is €7.00 per MWh, the participant who acquired the right incurs a loss of €0.25 per MWh. This loss occurs because the holder is obligated to pay €7.25 for each hour of using the rights, regardless of whether the price spread is favorable or unfavorable.

The marginal price of the auction can be considered the option premium. However, this premium may not always reflect the market value of the option, leading to what is known as underpricing or overvaluation, depending on the situation.

Underpricing occurs when the auction premium is systematically lower than the true economic value of the option. For example, if the marginal price of the FTR option in an auction is €10 per MWh , but the actual value of securing transmission capacity based on the average price spreads is €15 per MWh, then the FTR option is considered underpriced. In this scenario buyers benefit from acquiring capacity at a lower cost than its true worth.

Conversely, overvaluation occurs when the auction premium exceeds the true economic value of the option. For instance, if the auction marginal price for the FTR option is set at €20 per MWh, but the actual value of the transmission rights, given market conditions, is only €15 per MWh, then the option is overvalued. In this case, buyers are paying more for the transmission capacity than its true economic value, leading to higher costs for acquiring the rights.

It becomes obvious that accurately modeling the fair value of FTR options becomes critical for market participants when placing bids in auctions for these rights. A precise valuation allows participants to make informed bidding decisions, ensuring that the auction marginal price reflects the true economic value of the congestion income.

3 Spread Option Tool

The second phase of the internship was to work closely with Margrabe's model for spread options. This included developing a Python tool for its implementation within the context of interconnection options.

Spread options have various applications in financial markets, particularly in commodity trading. As detailed in Carmona & Durrleman (2003), the authors explain that these options can be based on:

1. the differences between the prices of the same commodity at two different locations (location spreads);

2. the differences between the prices of the same commodity at two different points in time (calendar spreads);

3. the differences between the prices of inputs to, and outputs from, a production process (processing spreads);

4. the differences between the prices of different grades of the same commodity (quality spreads).

3.1 Margrabe's Model

The analysis of spread options often examines the special case where the strike price $K = 0$. Consider two indices, $S_1 = \{S_1(t)\}_{t \geq 0}$ and $S_2 = \{S_2(t)\}_{t \geq 0}$, which can represent prices of stocks, commodities, or other financial metrics like interest or exchange rates. When both S_1 and S_2 follow log-normal distributions, a closed-form pricing solution, analogous to the Black-Scholes formula, can be applied. This solution, commonly known as *Margrabe's formula*, was first introduced in his 1978 paper Margrabe (1978).

As mentioned by René Carmona and Valdo Durrleman in Carmona & Durrleman (2003), the case $K = 0$ corresponds to an exchange option, where the payoff is given by $S_2(T) - S_1(T)$. This option grants the holder the right to receive the difference $S_2(T) - S_1(T)$ at maturity T, effectively providing a means to profit from the spread between S_2 and S_1.

To illustrate this, consider an FTR option. By acquiring such an option, the holder benefits whenever the hourly spread between two locations is positive, mirroring the strategy of buying a bundle of options to exchange S_1 for S_2 if one anticipates that S_2 will outperform S_1.

In this context, FTRs can be viewed as a bundle of exchange options that are specifically written on the spot spread price between interconnected power markets.

3.2 Model Assumptions and Close Form Solution

In this section, the key assumptions of the model are outlined and the closed-form solution is presented. Instead of deriving the full formulas, the focus is on highlighting the fundamental concepts and main ideas behind Margrabe's model. Carmona and Durrleman Carmona & Durrleman (2003) provide a detailed derivation of the complete model.

To begin with the methodology, the authors describe the risk-neutral dynamics of the two underlying indices as following Geometric Brownian Motions, expressed as:

$$\frac{dS_i(t)}{S_i(t)} = r dt + \sigma_i dW_i(t), \quad i = 1, 2, \tag{1}$$

where $\{W_1(t)\}_t$ and $\{W_2(t)\}_t$ are Brownian Motions with a correlation ρ, ranging from -1 to 1. Specifically, these Brownian Motions are defined as:

$$W_1(t) = \rho \tilde{W}_1(t) + \sqrt{1 - \rho^2} \tilde{W}_2(t) \quad \text{and} \quad W_2(t) = \tilde{W}_1(t),$$

where $\{\tilde{W}_1(t)\}_t$ and $\{\tilde{W}_2(t)\}_t$ are independent Standard Brownian Motions.
The parameter ρ controls the correlation between the two indices, derived from the expectation:

$$\mathbb{E}[dW_1(t)dW_2(t)] = \rho\, dt.$$

Moreover, parameters σ_1 and σ_2 represent the individual volatilities of both indices and r represents the rate of interest. All these parameters are assumed to be constant.
The explicit solutions for the indices are:

$$S_i(t) = S_i(0) \exp\left[\left(r - \frac{\sigma_i^2}{2}\right) t + \sigma_i W_i(t)\right], \quad i = 1, 2. \tag{2}$$

Given the payoff of a spread option defined as:

$$\max\{S_1(t) - S_2(t) - K, 0\}.$$

It can be proved that the closed-form solution for the exchange option price p, with strike $K = 0$ and maturity T is given by:

$$p = S_2(0)\Phi(d_1) - S_1(0)\Phi(d_2), \tag{3}$$

where

$$d_1 = \frac{\ln(S_2(0)/S_1(0))}{\sigma\sqrt{T}} + \frac{1}{2}\sigma\sqrt{T}, \tag{4}$$

$$d_2 = \frac{\ln(S_2(0)/S_1(0))}{\sigma\sqrt{T}} - \frac{1}{2}\sigma\sqrt{T}. \tag{5}$$

To account for how the two underlying assets move in relation to each other, Margrabe uses the combined volatility σ^2, defined as :

$$\sigma^2 = \sigma_1^2 - 2\rho\sigma_1\sigma_2 + \sigma_2^2. \tag{6}$$

This combines the individual volatilities of the assets and adjusts for their correlation. If the assets move together in a similar pattern (high positive correlation), the combined volatility will be lower than if they move in opposite directions (high negative correlation). This combined volatility is crucial for accurately pricing the spread option, as it reflects the overall uncertainty of the spread between the two assets.

The Delta, or the first derivative of the option price with respect to the underlying asset, is given by:

$$\frac{\partial p}{\partial S_1} = \Phi(d_1), \tag{7}$$

and similarly for S_2:

$$\frac{\partial p}{\partial S_2} = -\Phi(d_2). \tag{8}$$

The symbol Φ represents the cumulative distribution function of the standard normal distribution.

3.3 FTR option tool implementation with Margrabe formula

The interconnection option between Spain and France is classified as a PTR with 'UIOSI'. For the sake of simplicity, this option will be referred to as a FTR, since under the 'UIOSI' mechanism, unused PTRs are effectively converted into FTRs.

Consequently, to determine the value of a monthly FTR option between Spain and France during the internship, futures prices for both locations were used as inputs for the indices (S_1 and S_2) in Margrabe's formula. The quotation date for the futures price aligns with the day of the option's calculation, and its maturity coincides with that of the FTR option, which is set at one month. This approach is based on the well-established economic principle that futures prices serve as reliable predictors of spot prices.

Furthermore, the annualized parameters for volatility and correlation of the futures prices were derived from the historical volatility and correlation of the log returns observed over a time series of the 90 days preceding the calculation date. These calculations assumed 360 trading days per year to ensure consistent annualization of the parameters.

The calculations of the monthly FTR option price involved computing the bundle of 744 hourly option values for the specific month, using the formula, where each option's maturity T corresponded to the number of days annualized from the day the option was calculated, until each of the 744 hours within the period. Subsequently, the mean of all the hourly option values was computed, obtaining the FTR option value in €/MWh, in line with standard practices in electricity markets where this option prices are typically quoted per MWh.

The results for the FTR options using the Margrabe formula could not be included in this work due to Energias de Portugal's data rights.

4 Stochastic Model for Spread Option

This chapter, corresponds to the final stage of the internship. The implementation of a spread option price model is presented, which will serve as the foundation for computing the FTR spread option value for the interconnections Spain $\rightarrow$ France and France $\rightarrow$ Spain.

4.1 Literature Review

This section reviews the literature on electricity markets, risk-neutral and real option pricing and interconnectors.

Many authors model electricity prices using a fundamental, structural approach based on production inputs. Barlow in Barlow (2002) develops a supply and demand model to obtain a diffusion model for electricity spot prices that can account for price spikes, which are an important empirical feature of electricity markets.

Kiesel and Kustermann Kiesel & Kustermann (2016) calibrate their structural model to the French-German electricity market area, analyzing the effects of market coupling on electricity prices, power plant valuation, and spread options. They find that market coupling can result in lower futures prices in all interconnected markets due to the convexity of the supply curve. Additionally, they observe that market coupling can lead to volatility spillover, where the introduction of an interconnector increases volatility in markets that were previously more stable

Coulon and Howison in Howison & Coulon (2009) develop a fundamental model for spot electricity prices, based on stochastic processes for underlying factors (fuel prices, power demand and generation capacity availability), as well as a parametric form for the bid stack function which maps these price drivers to the power price.

Abadie and Chamorro in Abadie & Chamorro (2021) provide an in-depth evaluation of the economic implications of cross-border electricity transmission interconnectors, focusing specifically on the Spain-France interconnector. They develop a stochastic model for the electricity spot price to analyze potential revenues resulting from the interconnector, accounting for features such as mean-reversion, seasonality, and price jumps in correlated domestic spot prices. The model incorporates an econometric approach to simulate revenue potentials based on actual electricity flows in both directions.

Regarding spread option pricing, Carmona & Durrleman (2003) provide a comprehensive review of the challenges associated with pricing and hedging spread options under the risk neutral setting. Their analysis is particularly focused on energy markets, where they delve into the numerical complexities encountered when applying various widely-used pricing models. Specifically, Carmona and Durrleman argue that the difference of two lognormal random variables can be approximated reasonably well by a normal random variable. This implies analytical pricing formulas which can be used for approximating the price of a spread option written on the difference between two commodities. More specifically, options written on the difference of two geometric Brownian motions, or two exponential Ornstein-Uhlenbeck processes driven by Brownian motions, may be approximated by a pricing formula derived from a normal distribution. Benth et al. (2008) focus on methodologies for accurately pricing and hedging options within energy markets also under the risk-neutral valuation framework. Chapter 9 in particular, discusses the valuation of exotic options in the energy market. It includes topics such as spread options, asian options, and provides a case study on spark spread options. This chapter aims to model and analyze these options with a particular emphasis on their empirical application, such as in the UK gas and electricity markets

The other literature that is relevant for the pricing of spread options in energy commodities under the risk neutral pricing framework is: Dempster et al. (2022), Hikspoors & Jaimungal (2007) and Marckhoff & Muck (2009).

Specifically for the case of interconnection options under the real option framework, Parmeshwaran & Muthuraman (2009) employ the loss-less Direct Current model to price Financial Transmission Rights options. The model simulates congestion scenarios in the transmission network, evaluates the resulting costs, and calculates the FTR option's value based on the difference between congestion and normal operating costs.

Álvaro Cartea and Carlos González-Pedraz, in Cartea & González-Pedraz (2012), take a real options approach to determine the value of an interconnector. They study five pairs of neighbouring European markets, determine the values of the interconnectors for each pair over a one-year period in their setup, and find that jumps in price spreads can have a significant impact on these values.

Let $S_{A,B}(t) = S_A(t) - S_B(t)$ denote the spread in wholesale prices at time t between locations A and B. The authors propose, under the statistical measure, the following arithmetic model for the price differences between locations A and B, $S^{A,B}(T)$, at time T:

$$S^{A,B}(T) = f(T) + X(T) + Y(T), \tag{9}$$

where $f(T)$ is a deterministic seasonal pattern (i.e., the long-term trend of the spot price) evaluated at time T, $X(T)$ is a mean-reverting stochastic process given by

$$X(T) = X(t)e^{-\alpha(T-t)} + \int_t^T e^{-\alpha(T-u)}\sigma(u)\, dW(u), \tag{10}$$

and $Y(T)$ is a zero-mean reverting pure jump process expressed as

$$Y(T) = Y(t)e^{-\beta(T-t)} + \int_t^T e^{-\beta(T-u)}\, dJ^+(u) + \int_t^T e^{-\beta(T-u)}\, dJ^-(u), \tag{11}$$

where α and β are the speeds of mean reversion for the Gaussian diffusion and the jump process, respectively. Here, $\sigma(t)$ represents the time-dependent deterministic volatility, $W(u)$ is a Standard Brownian Motion, and $J^+(u)$ and $J^-(u)$ are Compound Poisson processes defined as

$$J^s(t) = \sum_{n=1}^{N^s(t)} j_n^s, \quad s = +, - \tag{12}$$

where $N^s(t)$ denotes an inhomogeneous Poisson process with time-dependent intensity $\lambda^s(t)$. The random variables $\{j^s(1), j^s(2), \ldots, j^s(n)\}$ represent the sizes of the jumps in the spread process, which are i.i.d. and exponentially distributed with parameter η^s, so that the expected size of each jump is $\frac{1}{\eta^s}$. The authors, after developing the spread price model, proceed to compute the option values for the five pairs of neighboring European electricity markets using the Fourier Transform method

Erwan Pierre and Lorenz Schneider in Pierre & Schneider (2024), build upon the Cartea and González-Pedraz modeling framework to incorporate recent advancements in market coupling and interconnectors. They enhance the model by refining the resolution of electricity prices from a daily scale (peak and off-peak periods) to an hourly scale. Additionally, they introduce regime-switching mechanisms to better represent the dynamics of coupled and decoupled hours in the electricity market.

4.2 Data Information

This study utilizes day-ahead spot prices for Spain and France, as well as monthly futures prices for both regions. Additionally, it incorporates auction prices and specific details related to the auction process for bidirectional flows between Spain and France. The spot and futures prices for France were obtained from the European Power Exchange (EPEX SPOT). For Spain, the spot prices were sourced from the Iberian Electricity Market Operator - Spanish Pool (OMIP). Information on monthly auction prices and detailed specifications regarding the auction process for bidirectional flows between Spain and France were collected from the JAO website.

The behaviour of electricity prices in European wholesale markets has changed significantly in recent years. During the period of 2021-2022, electricity prices experienced a significant increase. According to Kuik et al. (2022) Kuik et al. (2022), the initial surge in energy prices in 2021 was primarily driven by the rebound in energy demand following the easing of lockdown measures from the first wave of the COVID-19 pandemic. The situation worsened in early 2022 with the onset of the Russian invasion of Ukraine causing an European gas crisis. Pierre and Schneider Pierre & Schneider (2024) also point that the low electricity production in France due to maintenance issues with nuclear power plants and the hot summer in 2021 were causes of the volatility in prices. Figure 3 illustrates the historical evolution of the hourly prices of the spread for the interconnection France $\rightarrow$ Spain from November 10th 2010 to May 31th 2024.

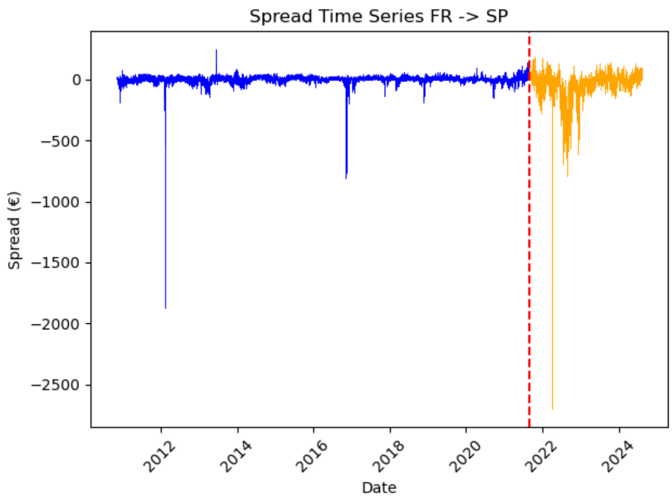

FIGURE 3: Historical hourly spread price for the interconnection FR $\rightarrow$ SP in Euros

As illustrated, volatility in the spread significantly increased from mid-2021 onwards, peaking at €2699.60 in hour 9 on April 3, 2022. Notably, even between 2010 and 2021, the time series of the spread shows substantial spikes and volatility, particularly in 2012 and 2016.

While there are significant spikes in the spread between years 2010 and 2021, this period can generally be characterized as stable. The fluctuations, although noteworthy, do not indicate the same level of volatility observed from mid-2021 onwards.

Given this recent fluctuations in electricity prices, analyzing a period with stable market conditions is crucial for accurate model estimation.

For reliable results, the focus is on the period from December 21, 2018, to November 24, 2020, due to its relative stability, which makes it ideal for assessing model performance. The dataset spans from November 9, 2012, to November 24, 2020.

4.3 Spread Option Modelling

To derive the fair value of the FTR option on the interconnection between Spain and France, the methodology used is based on the stochastic model designed by Cartea and González-Pedraz in Cartea & González-Pedraz (2012) under the real options framework. Several modifications have been made to simplify the model and enhance its tractability. First, the parameters α and σ are assumed to be constant. Additionally, the parameter β is set to be equal to α.

Furthermore, instead of modeling the jump component as a time-inhomogeneous Poisson process with time-dependent intensity, it is assumed that the Poisson process is homogeneous, thus, with a constant intensity λ^s. This assumption simplifies the jump process while maintaining the capability to model sudden and significant changes in the spread price.

Following the Cartea and González-Pedraz model, a framework is proposed for modeling electricity spreads under the physical probability measure $\mathbb{P}$. Let $(\Omega, \mathcal{A}, \mathbb{P}, \mathcal{F})$ represent a filtered probability space. Denote the electricity spot prices at time t in locations A and B by $S^A(t)$ and $S^B(t)$, respectively. The spread between these two prices is defined as:

$$S^{A,B}(t) = S^A(t) - S^B(t).$$

At time T:

$$S^{A,B}(T) = f(T) + X(T) + Y(T) \tag{13}$$

with,

$$X(T) = X(t)e^{-\alpha(T-t)} + \int_t^T e^{-\alpha(T-u)}\sigma \, dW_u, \tag{14}$$

$$Y(T) = Y(t)e^{-\alpha(T-t)} + \int_t^T e^{-\alpha(T-u)} \, dJ^+(u) + \int_t^T e^{-\alpha(T-u)} \, dJ^-(u), \tag{15}$$

where $f(T)$ is a deterministic seasonal pattern (i.e., the long-term trend of the spot) evaluated at time T, $X(T)$ is a mean-reverting stochastic process with a jump component at time T, α corresponds to the speed of mean reversion for the Gaussian diffusion and Jump component, σ is the deterministic volatility, $W(u)$ is a Standard Brownian Motion, and $J(u)^+$ and $J(u)^-$ are Compound Poisson processes, defined as:

$$J^s(t) = \sum_{n=1}^{N^s(t)} j_n^s, \quad s = +, - \tag{16}$$

where $N^s(t)$ denotes Poisson processes with constant intensities λ^s. The random variables $\{j^s(1), j^s(2), \ldots, j^s(n)\}$ represent the sizes of the jumps in the spread process, which are i.i.d. and exponentially distributed with parameters η^s, so that the expected sizes of each jump are $\frac{1}{\eta^s}$.

4.4 Option Valuation

When electricity is transferred between countries, the resulting spread can be expressed in two distinct ways, depending on the direction of the flow. For instance, FR $\rightarrow$ SP indicates electricity is transmitted from France (FR) to Spain (SP), meaning electricity is purchased in France and sold in Spain. This leads to a spread of:

$$S^{SP,FR} = S^{SP} - S^{FR}.$$

Conversely, SP $\rightarrow$ FR signifies electricity is sent from Spain to France, where electricity is bought in Spain and sold in France, producing the opposite spread:

$$S^{FR,SP} = S^{FR} - S^{SP}.$$

Having the spread price model, to determine the fair price of the FTR for the general interconnection direction $B \rightarrow A$, the formulas introduced by Erwan Pierre and Lorenz Schneider in Pierre & Schneider (2024) are applied. Specifically, the fair price is computed by averaging T_N hourly call options on the spread $S^{A,B}(t)$, where T_N represents the total number of hours in the contract period.

Conversely, for the reverse direction $A \rightarrow B$, the FTR is modeled as a put option on the $B \rightarrow A$ spread.

The model price of a single call option with strike $K^{A,B}$ at an hour T is given by the discounted expected payoff:

$$C^{A,B}(t, T, K^{A,B}) = e^{-r(T-t)} \mathbb{E}_t \left[\max \left\{ S^{A,B}(T) - K^{A,B}, 0 \right\} \right], \tag{17}$$

and the value of the monthly option is then given by:

$$C^M_{A,B}(t, T, K^{A,B}) = \sum_{T=T_1}^{T_N} C^{A,B}(t, T, K^{A,B}), \tag{18}$$

where $T_1, \ldots, T_N$ are the hours of delivery in month M and r is the continuously-compounded risk-free interest rate. In practice, the strike $K^{A,B}$ is usually set to zero. However, the formulation considers the more general case where any strike price is allowed. Non-zero strike values may account for factors such as interconnection fees, for example.

In line with standard practices in electricity markets, option prices are typically quoted per MWh. To calculate the option price aligned with the standard practices, the result from equation 18 is divided by the number of hours in the month:

$$\text{FTR value per MWh} = \frac{1}{T^N} C^M_{A,B}(t, T, K^{A,B}). \tag{19}$$

4.5 Implementation of The Spread Price Modelling

The time series of the spread between Spain and France was analyzed on an hourly basis from November 10, 2010, to November 24, 2020. Figure 4 presents this data, highlighting key patterns and behaviors in the hourly price differences over this period.

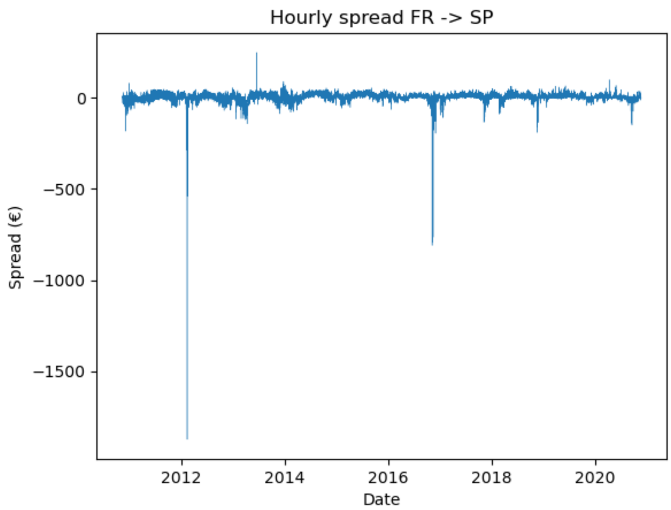

FIGURE 4: Price differentials "Spain minus France" with day ahead prices (2010-2020)

The mean level function to model the trend and seasonal component of the spot price was based on the approach developed in Cartea & González-Pedraz (2012), corresponding to:

$$f_t = f_0 + f_1 t + \sum_{m=1}^{11} F_m D_t^m.$$

In this discrete-time version of $f(t)$, f_0 represents a constant term, while f_1 is the coefficient associated with the time trend. The parameters F_m (for $m = 1, \ldots, 11$) are monthly constants, and the variables D_t^m are monthly dummy variables, which take the value of 1 if time t falls within the m-th month and 0 otherwise. Table I shows the estimated coefficients obtained using the `curve_fit` function from the SciPy library in Python for Non-Linear Least Squares regression.

Coefficient	Spain/France	
	Value	t-stat
f_0	3.26	14.38
f_1	-0.0027	-64.72
F_1 (January)	1.31	4.54
F_2 (February)	-2.16	-7.34
F_3 (March)	-3.30	-11.46
F_4 (April)	-0.95	-3.29
F_5 (May)	10.39	36.08
F_6 (June)	14.16	48.75,
F_7 (July)	12.63	43.86,
F_8 (August)	11.45	39.22
F_9 (September)	7.79	26.34
F_{10} (October)	5.85	19.93
F_{11} (November)	-3.85	-13.20
R^2	0.00245	-
F-stat	16.62	-
(p-value)	(0.000)	-

TABLE I: Coefficients Spain/France

The t-statistics for all the coefficients in the model are significantly higher in absolute value than the critical values associated with commonly used significance levels. Specifically, they exceed ± 1.645 for a 10% significance level, ± 1.96 for a 5% significance level, and ± 2.576 for a 1% significance level. This indicates that each coefficient is statistically significant across all these significance thresholds.

The null hypothesis of the F-test posits that all regression coefficients, except the intercept, are zero, suggesting that none of the predictors have a significant effect on the dependent variable. Given that the p-value is substantially smaller than standard significance thresholds and the F-statistic exceeds the critical values of 2.18, 1.75, and 1.55 at the 1%, 5%, and 10% significance levels, respectively, it can be concluded that at least one predictor in the model is statistically significant and contributes meaningfully to explaining the variance in the dependent variable.

Despite this, the R^2 value of 0.00245 indicates that only 0.245% of the variance in the dependent variable is explained by the predictors in the model. This extremely low value suggests that the model accounts for very little of the variability in the dependent variable, highlighting that while the predictors are statistically significant, the model's overall explanatory power is minimal. This finding is consistent with the results for the deterministic component reported in Cartea & González-Pedraz (2012).

Given that the independent variables have been shown to be statistically significant, the seasonality function is incorporated into the model to assess its effects.

Figure 5 showcases the seasonality function for the spread Spain/France, fitted to the entire period range of the dataset and the detrended and deseasonalized time series, providing insights into the underlying patterns after removing trends and seasonal effects.

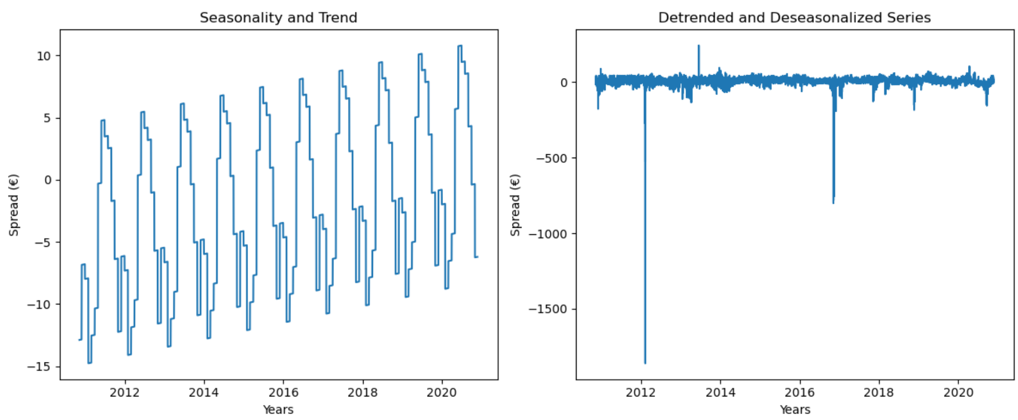

FIGURE 5: Seasonality function for Spain/France

The empirical Autocorrelation Function (ACF) and Partial Autocorrelation Function (PACF) of the detrended and deseasonalized time series, shown in Figure 6, indicate an autoregressive model of order 1: the ACF gradually declines, suggesting a diminishing correlation over successive lags; the PACF shows a significant spike at lag 1, with no notable correlation at higher lags.

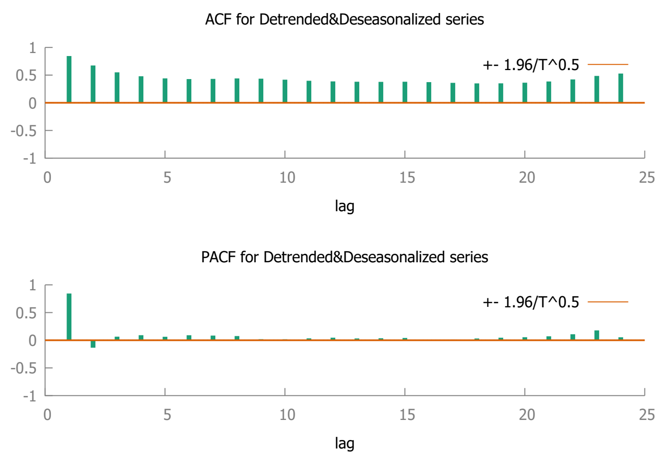

FIGURE 6: ACF and PACF of the detrended and deseasonalized time-series

Figure 7 illustrates the ACF and the PACF of the residuals derived from the fitted AR(1) model.

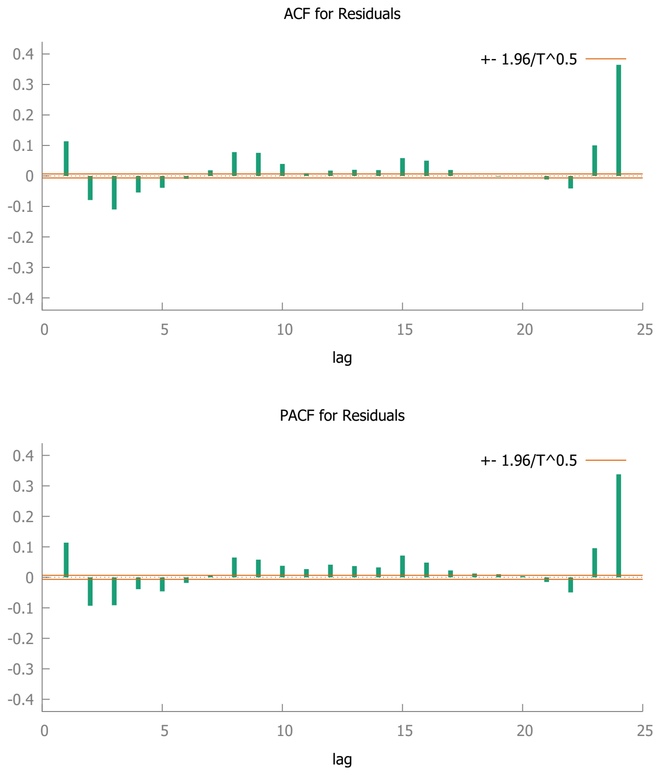

FIGURE 7: ACF and PACF of the adjusted AR(1) model

Given the influence of sample size on the boundaries in the ACF and PACF plots of Figure 7, and considering the large sample in this analysis, it is reasonable to assume the residuals are uncorrelated, as small correlations may appear significant but are typically considered negligible. Consequently, it is appropriate to proceed with the established AR(1) model. The coefficient of the AR(1) was estimated using `AutoReg` function from the Statmodels library in Python.

Defining the autoregressive model as the following equation:

$$z_{t+1} = \gamma z_t + \epsilon_t, \quad \hat{\gamma} = 0.8442,$$

with $\{\epsilon_t, t \in \mathbb{N}\}$ as an i.i.d. process, time measured on a discrete hourly scale, and the autoregression coefficient γ assumed to be constant, a connection can be made between this autoregressive model and the stochastic model.

Letting $Z(t) = X(t) + Y(t) = S^{A,B}(t) - f(t)$, then:

$$dS^{A,B}(t) - df(t) = -\alpha X(t)\,dt + \sigma\,dW(t) - \alpha Y(t)\,dt + dJ^{+}(t) + dJ^{-}(t)$$

$$\iff dZ(t) = -\alpha Z(t)\,dt + \sigma\,dW(t) + dJ^{+}(t) + dJ^{-}(t).$$

Discretizing this equation using hourly increments results in:

$$\Delta Z(t) \approx -\alpha Z(t) + \sigma \Delta W(t) + \Delta J^{+}(t) + \Delta J^{-}(t)$$

$$\iff Z(t+1) \approx (1-\alpha) Z(t) + \sigma \Delta W(t) + \Delta J^{+}(t) + \Delta J^{-}(t).$$

Given $\Delta W(t) = W(t+1) - W(t)$ and $\Delta J^{+-}(t) = J^{+-}(t+1) - J^{+-}(t)$, and considering the independence of the increments of a Brownian motion and of a Compound Poisson process, $\sigma \Delta W(t) + \Delta J^{+}(t) + \Delta J^{-}(t)$ forms an i.i.d. sequence for $t \in \mathbb{N}$.

Then, it is easy to check that this discretized version of $Z(t)$ coincides with the time series z_t, considering $\gamma \equiv 1 - \alpha$ and $\epsilon_t \equiv \sigma \Delta W(t) + \Delta J^{+-}(t)$.

The hourly estimate $\hat{\gamma} = 0.8442$ is significant at all usual significance levels. This estimate indicates that the hourly mean reversion speed is $\hat{\alpha} = 1 - \hat{\gamma} = 0.1558$.

The examination of the residuals from this model reveals substantial deviations from normality, supported by both statistical testing and visual analysis (see Figure 8).

The critical values for the Kolmogorov-Smirnov (K-S) test at the 1%, 5%, and 10% significance levels are approximately 0.0054, 0.0046, and 0.0041, respectively. Given that the K-S test statistic is 0.18389, which is above all these critical values, the null hypothesis of normality is rejected at all significance levels. Additionally, the p-value of 0.00 strongly indicates that the residuals significantly deviate from a normal distribution.

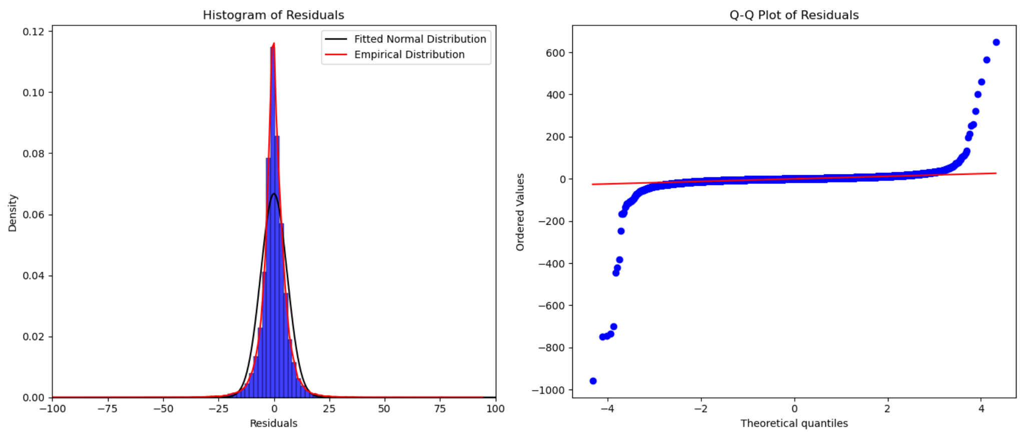

FIGURE 8: Histogram of the AR(1) residuals limited between -100 and 100 (left) and corresponding QQ-plot for normality (right).

The QQ-plot for normality indicates that the central part of the data, between quantiles -2 and 2, aligns well with the normal distribution, suggesting normality in this range. However, significant deviations from the normal distribution are observed in the extreme tails.

Specifically, the lower tail (from quantiles -4 to -2) and the upper tail (from quantiles 2 to 4) both show substantial deviations, indicating that the tails of the distribution are heavier and contain more extreme values than what would be expected under a normal distribution. These notable deviations suggest the presence of jumps within the residuals. To address this issue, it is necessary to systematically identify and quantify these deviations in order to refine the model. By isolating the jumps, the model defined by equations 20, 21, and 22, which is designed to distinguish jumps from normal residual variations, can be effectively implemented.

To detect this jumps in the time series, a recursive filtering procedure outlined by Clewton and Strickland Clewlow & Strickland (1999) is employed, as summarized in Algorithm 1 below:

Algorithm 1 Jump Detection Algorithm

1: Calculate the mean and the standard deviation of the time series;
2: Identify as a jump any data point that deviates from the mean by more than two to three times the standard deviation;
3: If no jumps are identified, then terminate the algorithm. Otherwise, remove the identified jumps and repeat from step 1;

Considering a threshold of 2.5 times the standard deviation to define jumps, and using the time series of the spread differences as the input, the algorithm converged after 14 iterations, with select iterations detailed in Table II.

The standard deviation obtained from the final iteration will serve as the estimate for the volatility in the process $\{X(t), t > 0\}$, resulting in an hourly volatility, $\sigma = 3.53$.

TABLE II: Jump identification and removal - recursive filtering procedure.

Iteration	Mean	SD	#PosJumps	#NegJumps	#TotalJumps	#CumulPosJumps	#CumulNegJumps	#CumulTotalJumps
1	-0.02654	5.17389	335	264	599	335	264	599
2	-0.04246	4.19543	1474	1407	2881	1809	1671	3480
3	-0.04720	3.80924	1104	1075	2179	2913	2746	5659
⋮	⋮	⋮	⋮	⋮	⋮	⋮	⋮	⋮
12	-0.02848	3.33441	15	23	38	4671	4666	9337
13	-0.02763	3.33151	9	17	26	4680	4683	9363
14	-0.02647	3.33028	0	11	11	4680	4700	9374

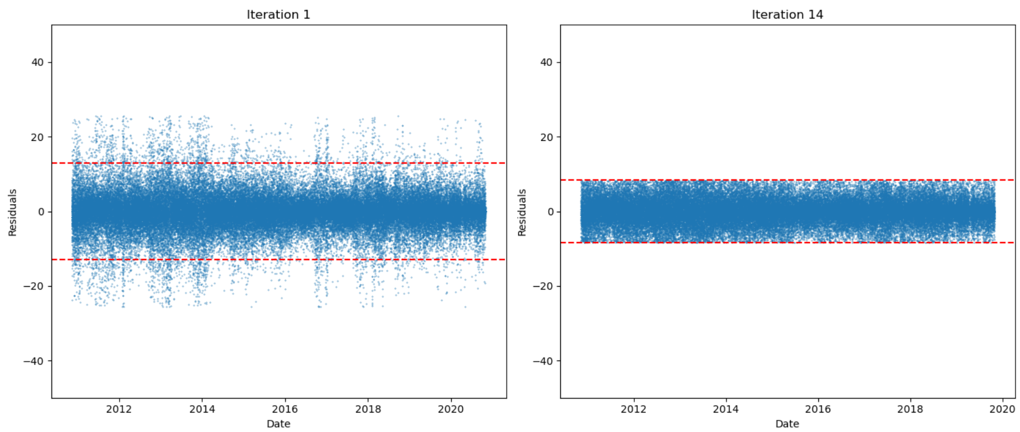

FIGURE 9: Identification of normal variations using the recursive filtering procedure

To assess the normality of the filtered residuals, a histogram of the residuals of the AR(1) after the jump removal (left) and a QQ-plot (right) for normality are examined in Figure 10.

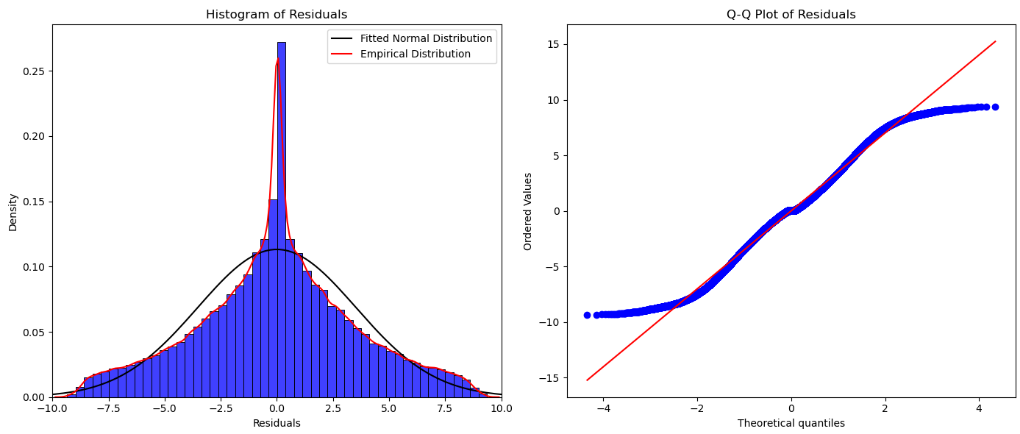

FIGURE 10: Identification of normal variations using the recursive filtering procedure

The critical values for the Kolmogorov-Smirnov (K-S) test at the 1%, 5%, and 10% significance levels are approximately 0.0058, 0.0049, and 0.0043, respectively. Given that the K-S test statistic is 0.03522 (greater than all critical values) and the p-value is 0.00, the null hypothesis of normality is rejected at all significance levels.
After removing the jumps, the QQ-plot reveals that while there are still heavy tails in both the upper and lower extremes, there are no significant outliers deviating substantially from the normal distribution. This indicates that the overall distribution of the data has been improved and better aligns with normality, even though the tails remain heavier than what a normal distribution would predict.

4.6 Compound Poisson process parameters

The intensities of the Poisson process can be obtained from Table II, in which the hourly jump frequencies were calculated dividing the total number of jumps by the total number of hours in the data set (87,983 hours), resulting in the following values:

$$\hat{\lambda}^{-} = 0.05322 \quad \text{and} \quad \hat{\lambda}^{+} = 0.05319.$$

The exponential distribution was adjusted to account for shifts of k^{+} units to the right for positive jumps, and k^{-} units to the right for negative jumps. This adjustment is necessary because, to model the jumps, only variations exceeding twice the mean were considered. Without this shift, the exponential distribution would include values representing normal variations, rendering the calculations redundant.

In Figure 11, the shifted distribution of the positive and negative jumps, shifted by k^{+-} units is shown. To model the negative jumps, their absolute values were considered, allowing them to be treated similarly to the positive jumps.

In this way:

$$k^{-} = 8.36 \quad \text{and} \quad k^{+} = 8.30.$$

The density function of a shifted exponential distribution (k units to the right) is given by:

$$f(x; \delta, k) = \eta e^{-\eta(x-k)}, \ i.e. \ , \ X - k \sim Exp(\eta).$$

Given a random sample $(X_1, ..., X_n)$, the estimator for δ is obtained using a maximum likelihood estimation (MLE):

$$\eta_{MLE} = \frac{1}{\bar{X} - k}.$$

This leads to the fitting in Figure 11, where the values for the negative and positive jumps are determined using the `stats.expon.fit` function from the SciPy library in Python and are given by:

$$\hat{\eta}^{-} = 0.1549 \quad \text{and} \quad \hat{\eta}^{+} = 0.1431.$$

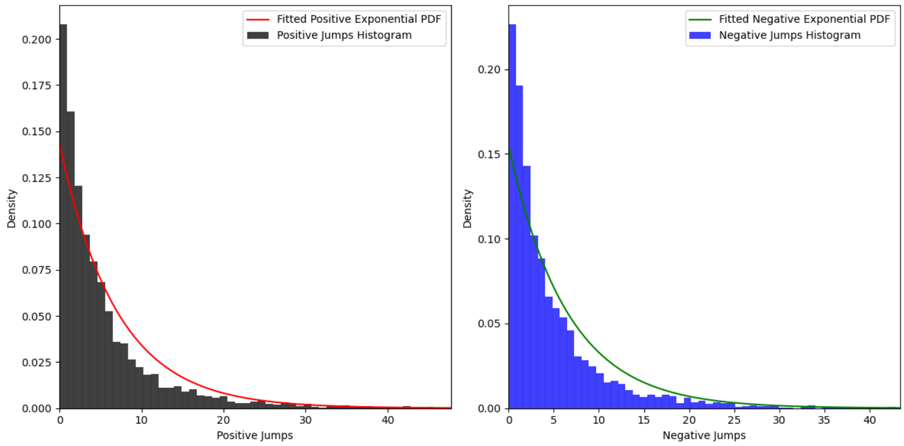

FIGURE 11: Histogram of positive and negative jumps with the fitted shifted exponential distribution

4.7 Backtesting

To validate the model's predictive performance, a backtesting procedure was conducted over the period from December 21, 2018, to November 24, 2020. This timeframe was selected due to its relatively stable fluctuations, making it well-suited for evaluating the model's performance.

In the model, the option value is determined on the auction's bid close date, the final day of the auction. To enhance performance, the model was adjusted by calibrating the jump and diffusion parameters using data from the past three months, while the seasonality function was calibrated using data from the last three years, for each calculation date. This calibration ensures a more responsive and up-to-date model. Regarding the other parameters, the risk-free rate r is set to the 2018 12-month Euribor at -0.186%, and the strike price K is set to zero. Additionally, it is assumed that the initial conditions of the diffusion and jump process are zero, i.e., $X(0) = 0$, $Y(0) = 0$.

The options were computed by doing a significant amount of simulations of the spread prices, for instance 1000 simulations were made for the maturity of 1 month, using ΔT = $\frac{1}{8640}$, thus making each time interval equal to an hour. Given that the maturity period desired is one month, the time to maturity (T) is expressed in years as: T = $\frac{1}{12}$.
Since the price of the spread option makes use of the Expected Value operator ($\mathbb{E}[\cdot]$), the following estimator was utilized:

$$\mathbb{E}[X] \approx \frac{1}{N} \sum_{i=1}^{N} x_i.$$

As such, the estimator for the spread option price, calculated at $t = 0$, using m paths, with maturity at an hour T, will be given by:

$$C^{A,B}(0,T,K^{A,B}) \approx \frac{exp(-rT)}{m}\left[\sum_{i=1}^{m} max\{S_T^{(i)} - K, 0\}\right],$$

where $S_T^{(i)}$ stands for the path number i that was simulated. Then, the result in €/MWh for the spread option price is obtained by applying equations 18 and 19.

It's important to note that the premium from the FTR auction represents the auction marginal price itself. The goal is to calculate the fair price of the FTR based on the average of the positive spreads over the month. This analysis allows market participants to make informed bids in the auction market. For instance, consider a market participant who relies on the model's predictions to develop his bidding strategy. If bids from other participants exceed the model's pricing, this participant risks not securing the rights, as the auction mechanism awards rights to those willing to pay the highest amounts. In this situation, the option premium may surpass the model's predictions. If the model's pricing is accurate, it indicates that the FTR option is overvalued in the market. Consequently, the participant would benefit from not winning the bid, as the overvaluation justifies avoiding the acquisition of transmission rights.

Figures 12 and 13 present a comparative analysis of the average of the positive spreads over the month, referred to as the 'Realized Premium', and model-predicted values for the period considered, covering both interconnections $FR \rightarrow SP$ and $SP \rightarrow FR$.

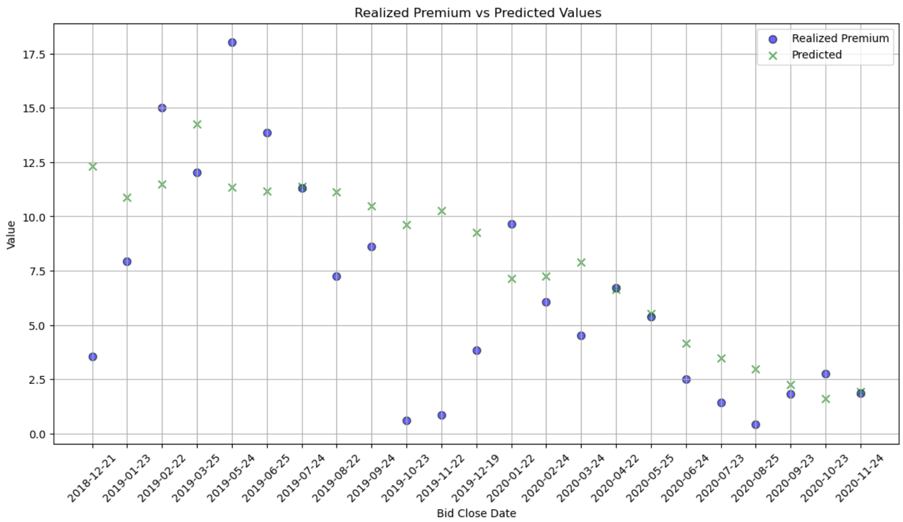

FIGURE 12: Comparison between Realized Premium and Predicted Option Premiums for interconnection FR $\rightarrow$ SP

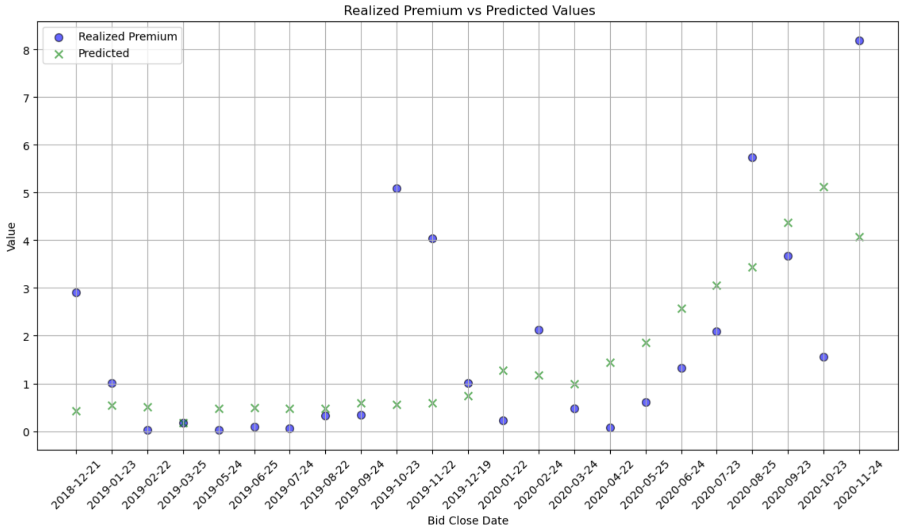

FIGURE 13: Comparison between Realized Premium and Predicted Option Premiums for interconnection SP $\rightarrow$ FR

Then, to better understand the predicative capabilities of the estimated model, the average absolute error as a percentage of the mean price (APE) and the root square mean error (RSME) were calculated for the period considered. The results are shown bellow

RMSE		**APE(%)**	
SP$\rightarrow$ FR	**FR $\rightarrow$ SP**	**SP$\rightarrow$ FR**	**FR$\rightarrow$ SP**
1.90	4.13	76.21	48.88

The results obtained were not satisfactory. The APE values, approximately 48.88% and 76.21% for both spreads, demonstrate that the model lacks precision in predicting spread option prices. Such high APE values suggest significant discrepancies between the predicted prices and Realized Premium, indicating that the model fails to capture the underlying market dynamics accurately. Additionally, RMSE values, around €4.13 and €1.90, imply that, on average, the model's predictions deviate from the actual values by these amounts.

In summary, the predicted prices are clearly far from aligning with market values. To enhance the model's predictive accuracy, further improvements and refinements will be implemented.

5 New Methodology

One of the key challenges identified in the current model is its reliance on an inadequate trend and seasonality function. As previously discussed, although the coefficients of the seasonality function are statistically significant at all significance levels, the low R-squared value indicates that this function does not adequately capture the variability in the spread.

It is well known that electricity prices exhibit seasonality across multiple frequencies, including daily, weekly, monthly, and yearly patterns. However, according to Pierre & Schneider (2024), seasonality has less impact on electricity price spreads between neighboring countries, as they often share similar consumption patterns. Additionally, during periods of market coupling, when cross-border trading is optimized, the price spread can reduce to zero, rendering seasonality irrelevant.

Spain and France are neighboring countries that frequently experience periods of market coupling and share many consumption patterns. Consequently, seasonal fluctuations in electricity prices between these two markets tend to cancel out to a large extent.

Furthermore, the authors point out that the market provides information on prices at a monthly granularity at the time of the auctions. This implies that, when pricing monthly spread options, there is only a constant view of the spread for the given period.

Consequently, in order to improve the accuracy of the model, the proposed approach involves using the market future prices that are relevant for the option period. When pricing monthly spread options, the new methodology will use the difference between the two monthly futures price of the countries involved as input. Thus, this new methodology eliminates the explicit trend and seasonality function from the spread price model and incorporates a long-term average parameter derived from the futures spread between the countries. This adjustment aligns with the assumption that the future spread price is a good predictor of the spot spread prices for electricity.

The revised formulation of the model is presented below:

$$S^{A,B}(T) = X(T) + Y(T), \tag{20}$$

with,

$$X(T) = X(t)e^{-\alpha(T-t)} + \int_t^T e^{-\alpha(T-u)}\mu\, du + \int_t^T e^{-\alpha(T-u)}\sigma\, dW_u, \tag{21}$$

$$Y(T) = Y(t)e^{-\alpha(T-t)} + \int_t^T e^{-\alpha(T-u)}\, dJ^+(u) + \int_t^T e^{-\alpha(T-u)}\, dJ^-(u). \tag{22}$$

In this formulation, μ represents the long-term average parameter associated with the futures price spread and is assumed to be constant. The remaining parameters and underlying assumptions align with those introduced in the initial methodology (See Section 4.3).

Furthermore, the methodology for determining jump process parameters, volatility and the speed of mean reversion remain consistent throughout the analysis as well as the formulas for pricing the option. However, since with this new methodology there is no seasonality function, the trend and seasonality were not removed from the time-series of the spread to estimate the parameters.

5.1 Backtesting of the new methodology

Similar to the initial methodology, the model parameters for both jump and diffusion processes were calibrated using data from the preceding three months, the parameter r was set to the 2018 12-month Euribor at -0.186% and the strike price K was set to zero. The futures spread utilized corresponds to the quotation date aligned with the bid close date of the auction. The maturity of this futures spread coincides with the maturity of the FTR option, set at one month. Table III provides a comprehensive overview of all auctions conducted over the specified period. It includes the marginal prices along with the market futures quotations for each country and corresponding spread futures. Additionally, the table presents the Realized Premiums and the predicted option prices according to the new methodology, specifically for both interconnections SP $\rightarrow$ FR and FR $\rightarrow$ SP.

JAO Auctions	**Auction (€ MW/h)**		**Market Futures**			**Realized Premium (€ MW/h)**		**New Model Predictions (€ MW/h)**	
Closing Date	**SP $\rightarrow$ FR**	**FR $\rightarrow$ SP**	**SP**	**FR**	**Spread**	**SP $\rightarrow$ FR**	**FR $\rightarrow$ SP**	**SP $\rightarrow$ FR**	**FR $\rightarrow$ SP**
December 21, 2018	12.49	1.76	65.00	76.50	11.5	2.92	3.54	11.55	0.03
January 23, 2019	7.44	2.07	62.08	69.25	8.45	1.02	7.92	6.99	0.22
February 22, 2019	0.51	6.61	48.90	42.40	6.50	0.02	15.00	0.62	7.94
March 25, 2019	0.32	9.6	46.75	36.65	10.10	0.17	12.01	0.29	10.96
April 26, 2019	0.14	14.05	52.30	37.65	14.65	0.17	11.22	0.11	14.90
May 24, 2019	0.14	11.69	48.55	36.70	11.85	0.02	18.02	0.21	12.03
June 25, 2019	0.11	0.00*	49.30	34.00	15.30	0.095	13.87	0.11	15.39
July 24, 2019	0.15	0.00*	51.00	37.65	13.35	0.06	11.33	0.13	13.32
August 22, 2019	0.21	7.89	45.50	38.40	7.10	0.32	7.24	0.63	7.74
September 24, 2019	1.71	4.86	48.18	45.10	3.08	0.33	8.62	1.33	4.52
October 23, 2019	3.51	3.89	52.10	52.85	0.75	5.08	0.59	3.01	2.03
November 22, 2019	3.00	3.62	49.50	49.10	0.40	4.04	0.84	2.53	2.33
December 19, 2019	6.21	1.92	46.57	51.50	4.93	1.01	3.84	6.02	0.25
January 22, 2020	1.43	5.00	41.50	38.00	3.50	0.23	9.65	0.32	3.71
February 24, 2020	1.95	3.08	32.75	31.00	1.75	2.13	6.07	1.17	3.19
March 24, 2020	1.26	4.91	22.98	18.90	4.08	0.47	4.52	0.98	4.95
April 22, 2020	1.08	4.31	22.20	18.10	3.5	0.08	6.70	0.78	4.95
May 25, 2020	0.46	4.16	26.15	22.75	3.40	0.60	5.37	0.71	4.17
June 24, 2020	0.71	2.54	36.38	34.90	1.48	1.32	2.51	0.89	2.62
July 23, 2020	0.71	3.55	34.80	32.25	2.55	2.08	1.44	0.62	3.43
August 25, 2020	2.26	1.36	40.00	41.20	1.20	5.74	0.41	1.81	0.60
September 23, 2020	3.56	1.43	41.55	43.75	2.20	3.68	1.81	2.48	0.14
October 23, 2020	4.42	1.66	45.45	48.60	3.15	1.56	2.76	3.86	0.15
November 24, 2020	2.22	2.59	42.15	42.35	0.20	8.19	1.87	1.67	0.95

TABLE III: Results and Data Summary. * Indicates instances where the auction was not executed.

Figures 14 and 15 present a comparative analysis of the actual FTR values (Realized Premium), and model-predicted values for the period considered.

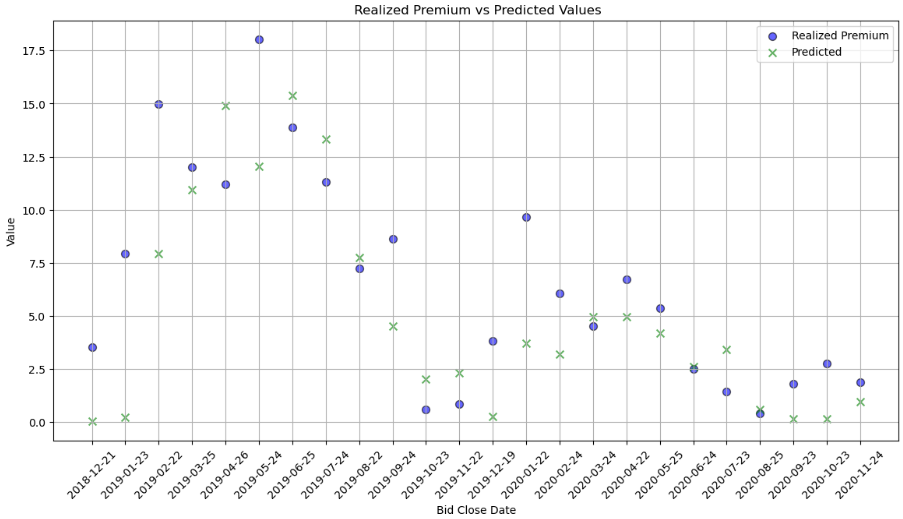

FIGURE 14: Comparison between Realized Premium and Predicted Option Premiums for interconnection FR $\rightarrow$ SP

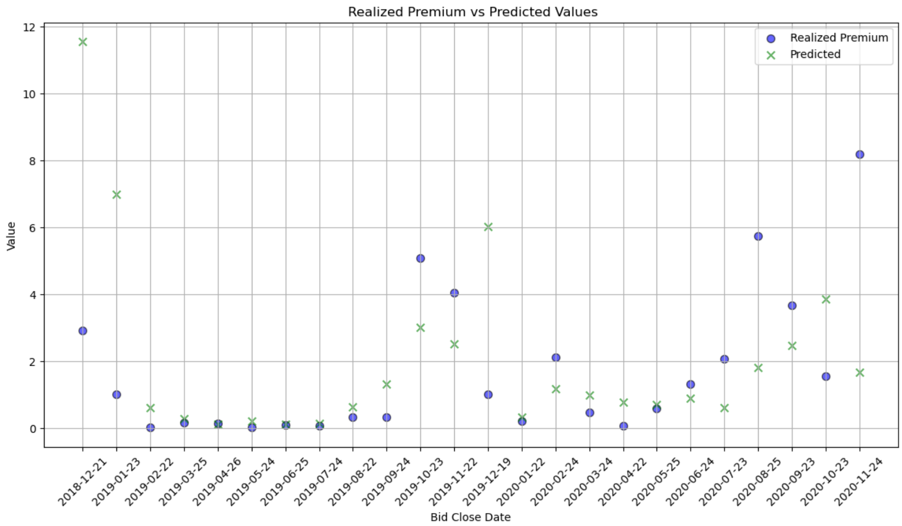

FIGURE 15: Comparison between Realized Premium and Predicted Option Premiums for interconnection SP $\rightarrow$ FR

The results for RMSE and APE are summarized below. These results indicate that the new methodology performs better in terms of accuracy for the FR $\rightarrow$ SP interconnection. However, it shows less favorable performance for the SP $\rightarrow$ FR interconnection, where the methodology yields higher errors in comparison with the first model. Overall, while the new approach demonstrates improvements in certain areas, it still falls short in accurately pricing spread options, suggesting that further refinement is needed to enhance its precision.

RMSE		APE(%)	
SP→ FR	**FR → SP**	**SP→ FR**	**FR→ SP**
2.66	3.21	104.34	37.48

With this new approach, a trading strategy can be developed by placing bids for monthly spread options in the JAO auction based on the model's estimated price. For simplicity, it is assumed that these bids do not affect the final auction price, which is reasonable when the bid volume is small compared to the total interconnection exchange volume. The strategy follows a straightforward rule: if the bid is successful, meaning the model's estimated price is higher than the auction price, a profit is achieved if the spread realized over the month exceeds the auction price at which the option was purchased; otherwise, a loss occurs. If the bid is too low and is not executed in the auction, the auction price is still compared with the realized spread to assess whether the lower bid was ultimately appropriate. Table IV presents these results.

JAO Auctions	Auction (€/MW/h)		Realized Premium (€/MW/h)		New Model Predictions (€/MW/h)		Trading Strategy P&L (€/MW/h)	
Closing Date	**SP → FR**	**FR → SP**	**SP → FR**	**FR → SP**	**SP → FR**	**FR → SP**	**SP → FR**	**FR → SP**
December 21, 2018	12.49	1.76	2.92	3.54	11.55	0.03	not exec	not exec
January 23, 2019	7.44	2.07	1.02	7.92	6.99	0.22	not exec	not exec
February 22, 2019	0.51	6.61	0.02	15.00	0.62	7.94	0.49	8.39
March 25, 2019	0.32	9.6	0.17	12.01	0.29	10.96	not exec	2.41
April 26, 2019	0.14	14.05	0.17	11.22	0.11	14.90	not exec	2.83
May 24, 2019	0.14	11.69	0.02	18.02	0.21	12.03	0.12	6.63
June 25, 2019	0.11	0.00*	0.095	13.87	0.11	15.39	0.015	-
July 24, 2019	0.15	0.00*	0.06	11.33	0.13	13.32	0.09	-
August 22, 2019	0.21	7.89	0.32	7.24	0.63	7.74	0.11	not exec
September 24, 2019	1.71	4.86	0.33	8.62	1.33	4.52	not exec	not exec
October 23, 2019	3.51	3.89	5.08	0.59	3.01	2.03	not exec	not exec
November 22, 2019	3.00	3.62	4.04	0.84	2.53	2.33	not exec	not exec
December 19, 2019	6.21	1.92	1.01	3.84	6.02	0.25	not exec	not exec
January 22, 2020	1.43	5.00	0.23	9.65	0.32	3.71	not exec	not exec
February 24, 2020	1.95	3.08	2.13	6.07	1.17	3.19	not exec	2.99
March 24, 2020	1.26	4.91	0.47	4.52	0.98	4.95	not exec	0.61
April 22, 2020	1.08	4.31	0.08	6.70	0.78	4.95	not exec	2.31
May 25, 2020	0.46	4.16	0.60	5.37	0.71	4.17	0.14	1.21
June 24, 2020	0.71	2.54	1.32	2.51	0.89	2.62	0.61	0.03
July 23, 2020	0.71	3.55	2.08	1.44	0.62	3.43	not exec	not exec
August 25, 2020	2.26	1.36	5.74	0.41	1.81	0.60	not exec	not exec
September 23, 2020	3.56	1.43	3.68	1.81	2.48	0.14	not exec	not exec
October 23, 2020	4.42	1.66	1.56	2.76	3.86	0.15	not exec	not exec
November 24, 2020	2.22	2.59	8.19	1.87	1.67	0.95	not exec	not exec

TABLE IV: Results of Trading Strategy. * Highlight the cases in which the auction failed to occur.

Assuming a capacity acquisition of 10 MW for each executed bid, this translates to an estimated profit of €146,959.20, calculated by multiplying the P&L for each executed bid by the total number of hours in the period and the acquired capacity, and then summing the results across all executed auctions. This highlights the critical role of capacity decisions in JAO auctions in determining a strategy's profitability. Thus, with a model delivering accurate predictions, the trading strategy has the potential to be highly profitable.

6 Conclusions

Several conclusions can be drawn from the backtesting performed for the two methodologies. Both models underperformed during the analysis period. Model 2 (New Methodology) outperformed Model 1 (First Model) for the interconnection FR $\rightarrow$ SP, while Model 1 showed better performance for the interconnection Spain $\rightarrow$ France. Although spread futures provide a forward-looking perspective on the spread spot price, their inclusion as a parameter primarily benefits the direction FR $\rightarrow$ SP, because the spread between Spain and France prices is typically positive, given that Spanish prices are generally higher. As a result, the realized spread for that direction in MWh for the month tends to be more predictable and closely aligns with the values of the spread futures. However, the seasonality function of Model 1 also proved unreliable. Due to market coupling in European markets and similar consumer patterns between Spain and France, stemming from the increasing integration of neighboring European countries, this seasonal behavior in spread spot prices tends to diminish. This inadequacy is evident in the model's seasonality function.

While trading and pricing spread options can be challenging in the volatile and uncertain electricity market, which limits the precision of the results from Models 1 and 2, these models still assist traders in making informed bidding decisions. Moreover, they outperform Margrabe's formula, which was the primary objective of developing them during the internship. Model 2 achieved an accuracy of 52.17% in its bidding strategy, successfully predicting whether options were underpriced or overpriced. Since the Model 1 has better predictions for the SP $\rightarrow$ FR interconnection, both models can be used for the trading strategy for each bidding direction. Although it was not tested, it could improve bidding decisions.

Future research could explore several compelling areas, including the development of a delta-hedging strategy to manage the risk associated with exposure to the financial derivative. This strategy would involve taking positions in the spread futures price between the two interconnection locations to achieve a delta-neutral portfolio. Additionally, future work could concentrate on estimating the β parameter of mean reversion within the jump component for both models, modeling the parameters of the diffusion and jump processes as time-dependent, as well as incorporating regime-switching mechanisms to more accurately capture the dynamics of coupled and decoupled hours. A closer examination of a new seasonality function, specifically tailored to the underlying patterns of electricity spot spread prices between Spain and France, could further refine the accuracy and predictive capabilities of Model 1.

REFERENCES

Abadie, L. M. & Chamorro, J. M. (2021), 'Evaluation of a cross-border electricity interconnection: The case of spain-france', *Energy* **233**, 121177.

Agency for the Cooperation of Energy Regulators (ACER) (2023), 'Acer decision on the harmonised allocation rules for long-term transmission rights: Annex i'.
URL: *https://www.jao.eu/resource-center/auction-rules*

Applebaum, D. (2009), *Levy Processes and Stochastic Calculus*, Vol. 116 of *Cambridge Studies in Advanced Mathematics*, Cambridge University Press.

Barlow, M. T. (2002), 'A diffusion model for electricity prices', *Mathematical finance* **12**(4), 287–298.

Benth, F. E., Benth, J. S. & Koekebakker, S. (2008), *Stochastic modelling of electricity and related markets*, Vol. 11, World Scientific.

Carmona, R. & Durrleman, V. (2003), 'Pricing and hedging spread options', *Siam Review* **45**(4), 627–685.

Cartea, Á. & González-Pedraz, C. (2012), 'How much should we pay for interconnecting electricity markets? a real options approach', *Energy Economics* **34**(1), 14–30.

Clewlow, L. & Strickland, C. (1999), A multi-factor model for energy derivatives, Technical report, Research Paper Series.
URL: *https://ideas.repec.org/p/uts/rpaper/28.html*

Dempster, M., Medova, E. & Tang, K. (2022), Long-term spread option valuation and hedging, *in* 'Commodities', Chapman and Hall/CRC, pp. 125–146.

Gautier, A. (2019), 'Eleclink: Shedding some light on a key european project'.
URL: *https://www.getlinkgroup.com/content/uploads/2019/12/191218-ElecLink-Study-uk-web.pdf*

Hikspoors, S. & Jaimungal, S. (2007), 'Energy spot price models and spread options pricing', *International Journal of Theoretical and Applied Finance* **10**(07), 1111–1135.

Hirth, L., Eicke, A. & Schlecht, I. (2024), 'An assessment of the status quo and proposed reforms of European long-term transmission rights'.
URL: *https://neon.energy/Neon-Forward-Markets.pdf*

Howison, S. & Coulon, M. (2009), ‘Stochastic behaviour of the electricity bid stack: from fundamental drivers to power prices’, *The Journal of Energy Markets* **2**, 29–69.

Kiesel, R. & Kustermann, M. (2016), ‘Structural models for coupled electricity markets’, *Journal of Commodity Markets* **3**(1), 16–38.

Kuik, F., Adolfsen, J. F., Meyler, A. & Lis, E. (2022), ‘Energy price developments in and out of the covid-19 pandemic–from commodity prices to consumer prices’, *Economic Bulletin Articles* **4**.

Marckhoff, J. & Muck, M. (2009), ‘Jump risk premia in short-term spread options: Evidence from the german electricity market’, *Available at SSRN 1403817* .

Margrabe, W. (1978), ‘The value of an option to exchange one asset for another’, *The Journal of Finance* **33**(1), 177–186.

Parmeshwaran, V. & Muthuraman, K. (2009), ‘Ftr-option formulation and pricing’, *Electric power systems research* **79**(7), 1164–1170.

Pierre, E. & Schneider, L. (2024), ‘Intermittently coupled electricity markets’, *Energy Economics* **130**, 107327.

APPENDICES

A FUNDAMENTAL CONCEPTS ABOUT INTERCONNECTION AUCTIONS

In this Appendix section, the fundamental notions and terminology necessary for understanding how interconnections between countries operate are defined, providing additional clarity and context where needed.

A.1 Market Time Unit (MTU)

The term 'Market Time Unit' refers to the duration for which the market price is set. It represents the shortest common time period used for pricing when the market time units of the two bidding zones differ.

A.2 Transmission System Operator (TSO)

Entities responsible for transporting energy in the form of natural gas or electrical power on a national or regional level, using fixed infrastructures.

TSOs manage the grid infrastructure and ensure the reliable delivery of energy. They also conduct auctions for the allocation of Long-Term Transmission Rights, such as Physical Transmission Rights and Financial Transmission Rights, which are used to manage and monetize grid capacity.

In Spain, the TSO is Red Eléctrica de España (REE), while in France, it is Réseau de Transport d'Électricité (RTE).

A.3 Single Allocation Platform

It is a service provider that facilitates the allocation of transmission capacity on behalf of multiple TSOs, handling the allocation and remuneration (payment) process for the transmission rights. Specifically, Joint Allocation Office (JAO) manages and conducts auctions for cross-border electricity transmission capacity in Europe.

A.4 Power Exchange

Platforms where electricity can be traded in large amounts. Companies like electricity producers and energy suppliers use the power exchange to sell their production and cover their demand (or the demand of their clients).

B Stochastic Processes

This appendix section introduces the theoretical background on stochastic processes, providing essential context for the concepts presented in this report.

B.1 Stochastic Process

Stochastic is, in simple words, something not deterministic (not predictable), thus being random. Stochastic Processes are families of random variables, whose purpose is to describe the evolution of a system. Stochastic processes can be classified based on the index set of the random variables. When the index set is countable, such as the set of natural numbers $\mathbb{N}$, the process is referred to as a discrete-time stochastic process. Conversely, if the index set is uncountable, such as the interval $T = [0, +\infty)$, the process is called a continuous-time stochastic process.

More theoretically, given a probability space $(\Omega, \mathcal{F}, P)$, a Stochastic Process is a collection $\{X_t : t \in T\}$ of random variables

$$X_t : \Omega \to \mathbb{R},$$

indexed by a parameter $t \in T \subseteq \mathbb{R}$.

Definition 1 (Stationary and Independent Increments) *A stochastic process X is said to be strictly (or strongly) stationary if*

$$(X_{t_1}, X_{t_2}, \dots, X_{t_n}) \stackrel{d}{=} (X_{t_1+h}, X_{t_2+h}, \dots, X_{t_n+h}), \tag{23}$$

for all possible choices of n; $t_1, t_2, \dots, t_n \in T$ and h.

A stochastic process X has stationary increments if

$$X_t - X_s \stackrel{d}{=} X_{t+h} - X_{s+h},$$

for all possible values of s,t and h.

It further has independent increments if the random variables

$$X_{t_2} - X_{t_1}, X_{t_3} - X_{t_2}, \dots, X_{t_n} - X_{t_{n-1}},$$

are independent whenever $t_1 < t_2 < \ldots < t_n$, $n \in \mathbb{N}$.

Definition 2 (Brownian Motion) *Brownian motion, also known as Wiener process, is a continuous-time stochastic process. In mathematical terms, $B = \{B_t : t \geq 0\}$, is a Brownian motion characterized by the following properties:*

1. $B_0 = 0$
2. *B has independent increments*
3. *If $s < t, B_t - B_s$ is a random variable with distribution N(0, t - s)*
4. *The process B has continuous trajectories*

Definition 3 (Lévy Measure) *Let ν be a Borel measure defined on $\mathbb{R}^d - \{0\}$. We say that ν is a Lévy measure if*

$$\int_{\mathbb{R}^d - \{0\}} (|x|^2 \wedge 1)\nu(dx) < \infty.$$

Definition 4 (Lévy Process) *Let X be a Stochastic Process. We say that X is a Lévy Process if*

1. $X(0) = 0$ *(a.s)* [1]
2. *X has independent and stationary increments*
3. *X is stochastically continuous, that is, for all $a > 0$ and for all $s \geq 0$*

$$\lim_{t \to s} \mathbb{P}(|X(t) - X(s)| > a) = 0.$$

A Lévy stochastic process consists of three key components: a deterministic function, a diffusion term, and a pure jump term. It is fully characterized by the Lévy triplet (γ,σ,ν), where γ represents the drift of the process, σ corresponds to the diffusion component, and ν is the Lévy measure that governs the behavior of the jump component (see Applebaum (2009)).

Definition 5 (Lévy-Khintchine formula) *If L is a Lévy process, then its characteristic function is given by*

$$\varphi_{L(t)}(u) = e^{t\eta_{L(1)}(u)},$$

with

$$\eta_{L(1)}(u) = i\mu u - \frac{1}{2}\sigma u^2 + \int_{\mathbb{R}\setminus\{0\}} \left(e^{iux} - 1 - iux\mathbf{1}_{\{|x|<1\}}(x)\right) \nu(dx).$$

$\eta_{L(1)}(u)$ is called the characteristic exponent of $L(1)$.

[1] The notion (a.s) stands for "almost surely", which is equivalent, in this case, to $\mathbb{P}[X(0) = 0] = 1$.

Definition 6 (Poisson process) *The Poisson process* $\{N(t),\ t \geq 0\}$ *with intensity* λ *has a characteristic exponent given by*

$$\eta_{N(1)}(u) = \lambda \left(e^{iu} - 1\right).$$

The Lévy triplet is given by

$$\left(0,\ 0,\ \lambda \mathbf{1}_{\{x=1\}}\, dx\right),$$

Definition 7 (Compound Poisson process) *The Compound Poisson (CP) process* $\{X(t) = \sum_{k=1}^{N(t)} Z_k,\ t \geq 0\}$*, where* $\{N(t),\ t \geq 0\}$ *is a Poisson process with intensity* λ *and the random variables* $Z_1, Z_2, \ldots$ *are i.i.d. with density function* $f_Z(x)$*, has a characteristic exponent given by*

$$\eta_{X(1)}(u) = \lambda \left(\varphi_Z(u) - 1\right),$$

where $\varphi_Z(u)$ *is the characteristic function of* Z*.*
The Lévy triplet is given by

$$\left(\int_{|x|\leq 1} x\nu(dx),\ 0,\ \lambda f_Z(x)\, dx\right).$$

Definition 8 (Ornstein-Uhlenbeck (OU) Process) *A càdlàg process* $\{X(t), s \leq t \leq T\}$ *is called an Ornstein-Uhlenbeck (OU) process if, for* μ*,* α*, and* σ *real-valued continuous functions on* $[0, T]$*, it is the unique strong solution of*

$$dX(t) = (\mu(t) - \alpha(t)X(t))dt + \sigma(t)dI(t), \quad X(s) = x.$$

The unique strong solution $\{X(t), s \leq t \leq T\}$ *is given by*

$$\begin{aligned} X(t) = &x \exp\left(-\int_s^t \alpha(\nu)d\nu\right) + \int_s^t \mu(u) \exp\left(-\int_u^t \alpha(\nu)d\nu\right) du \\ &+ \int_s^t \sigma(u) \exp\left(-\int_u^t \alpha(\nu)d\nu\right) dI(u). \end{aligned}$$

C Time-Series

Definition 9 (Autoregressive Process) *Considering a white noise $(Z_t) \sim WN(0, \sigma_Z^2)$, an autoregressive model of order p, denoted AR(p), is defined as:*

$$X_t = \sum_{i=1}^{p} \psi_i X_{t-i} + Z_t = \psi_1 X_{t-1} + \ldots + \psi_p X_{t-p} + Z_t.$$

Definition 10 (Autocorrelation Function) *The autocorrelation function at lag k, denoted ρ_k, of a stationary stochastic process y_t is given by:*

$$\rho_k = \frac{Cov(y_t, y_{t-k})}{Var(y_t)} = \frac{\gamma_k}{\gamma_0},$$

where $Cov(y_t, y_{t-k})$ is the covariance between the observations at times t and $t-k$, $Var(y_t)$ is the variance of y_t, γ_k is the covariance at lag k, and γ_0 is the variance at lag 0. The autocorrelation function provides information regarding the existing correlation between two observations k periods apart. This function can be interpreted as the memory of the process.

Definition 11 (Partial Autocorrelation Function) *The Partial Autocorrelation Function (PACF) at lag k, denoted as ϕ_{kk} is given by:*

$$\phi_{kk} = Corr(X_t, X_{t-k} \mid X_{t-1}, X_{t-2}, \ldots, X_{t-(k-1)}).$$

It quantifies the correlation between the time series X_t and its lagged values X_{t-k} after removing the effects of all intermediate lags. It is a crucial tool in time series analysis for determining the appropriate order of autoregressive models.

C.1 Error Measures

To calibrate and evaluate the performance of the models, some error measures were used, such as the root-mean-square error (RMSE) and the average absolute error as a percentage of the mean price (APE). These are defined as :

$$\text{RMSE} = \sqrt{\frac{1}{n}\sum_{i=1}^{n}(\text{market price}_i - \text{model price}_i)^2},$$

$$\text{APE} = \frac{\sum_{i=1}^{n} |\text{market price}_i - \text{model price}_i|}{\sum_{i=1}^{n} \text{market price}_i}.$$

D Statistical Tests

D.1 Kolmogorov-Smirnov Test

To check if some data follow a specified distribution, along with QQ-plots, the Kolmogorov-Smirnov test was used during this work. This test considers the following hypotheses:

- Null Hypothesis (H_0): The data follow a specified distribution.
- Alternative Hypothesis (H_1): The data do not follow a specified distribution.

E Simulations

The algorithms used to discretize the stochastic processes involved in the models will be introduced.

E.1 Price Process Simulation Model 1

The process $\{S(t), t \geq 0\}$ can be simulated by independently simulating the processes $\{X(t), t \geq 0\}$ and $\{Y(t), t \geq 0\}$, respectively.

For ease of notation, t is used in subscript to denote the discrete version of the continuous time variables, thus, the discrete versions of $X(t)$ and $Y(t)$ are denoted by X_t and Y_t, respectively.

The discrete-time evolution of X_t is modeled by:

$$X_t = e^{-\alpha \Delta t} X_{t-\Delta t} + \epsilon_t, \quad t = 1, 2, \ldots, N,$$

where ϵ_t represents the Brownian Motion increment at time t, with:

$$\mathbb{E}[\epsilon_t] = 0 \quad \text{and} \quad \mathbb{E}[\epsilon_t^2] = \sigma_{\epsilon,t}^2 = \frac{\sigma_t^2}{2\alpha}\left(1 - e^{-2\alpha \Delta t}\right).$$

This formulation arises from discretizing an Ornstein-Uhlenbeck process, where the mean-reversion speed is α and the diffusion coefficient is σ_t^2.

The discrete-time version of the jump process Y_t is modeled by:

$$Y_t = e^{-\beta \Delta t} Y_{t-\Delta t} + \Delta J^+ + \Delta J^-,$$

where ΔJ^+ and ΔJ^- represent the positive and negative jumps occurring at time t. These jumps are defined as:

$$\Delta J^+ = J^+ \Delta N^+ \quad \text{and} \quad \Delta J^- = J^- \Delta N^-,$$

with ΔN^+ and ΔN^- being the increments of the Poisson counting processes for positive and negative jumps, respectively. The arrival rates for these jumps are $\lambda^+ \Delta t$ and $\lambda^- \Delta t$. The jump sizes J^+ and J^- are independent and exponentially distributed random variables with means:

$$\mathbb{E}[J^+] = \frac{1}{\eta^+} \quad \text{and} \quad \mathbb{E}[J^-] = \frac{1}{\eta^-}.$$

Finally, S_t will be given by :

$$S_t = f_t + X_t + Y_t,$$

where f_t denotes the discretized form of the seasonality function $f(t)$, as previously discussed in Section 4.5.

In figures below, 10 hourly trajectories over a 30-day period are presented for the diffusion process X_t and the jump process Y_t, with parameters detailed in Section 4.5. The step size was set to $N = 30 \times 24 = 720$, representing the 720 hours in a month, and the time-to-maturity parameter was set to $T = \frac{1}{12}$, corresponding to a one-month period.

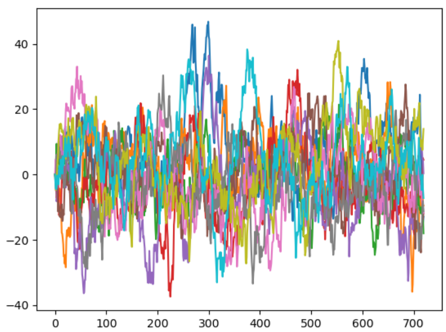

(a) X_t simulation for Model 1

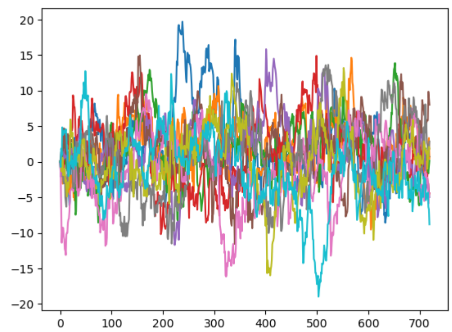

(b) Y_t simulation for Model 1

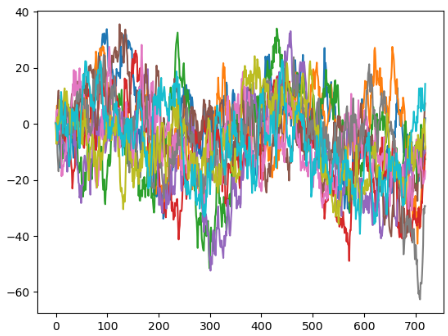

(c) S_t simulation for Model 1

E.2 Price Process Simulation Model 2

Again the process $\{S(t), t \geq 0\}$ can be simulated by independently simulating the processes $\{X(t), t \geq 0\}$ and $\{Y(t), t \geq 0\}$, respectively.

The discrete-time evolution of X_t is modeled by:

$$X_t = \mu + e^{-\alpha\Delta t}(X_{t-\Delta t} - \mu) + \epsilon_t, \quad t = 1, 2, \ldots, N,$$

where μ denotes the long-term average parameter and ϵ_t represents the Brownian motion increment at time t, as derived in the preceding subsection.

The discrete-time version of the jump process Y_t is modeled in the same way as in the previous subsection for both jump components. Finally, S_t will be given by :

$$S_t = X_t + Y_t.$$

In the figures below, 10 hourly trajectories over a 30-day period are shown for the diffusion process X_t and price process S_t. As the jump process is identical for both models, it is not displayed. The parameters are detailed in Section 4.5. The step size was set to $N = 30 \times 24 = 720$, and the time-to-maturity parameter was set to $T = \frac{1}{12}$, corresponding to one month. The drift parameter was chosen as $\mu = -60$.

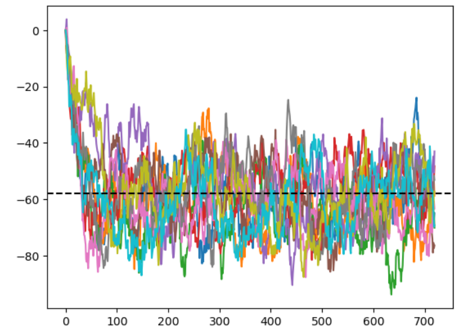

(a) X_t simulation for Model 2

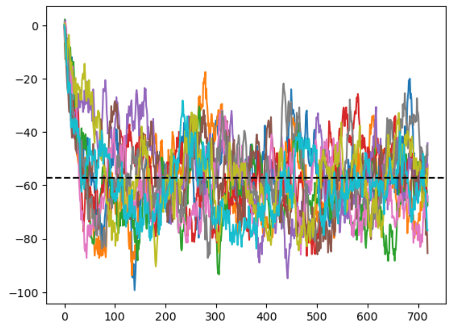

(b) S_t simulation for Model 2

F Additional Data

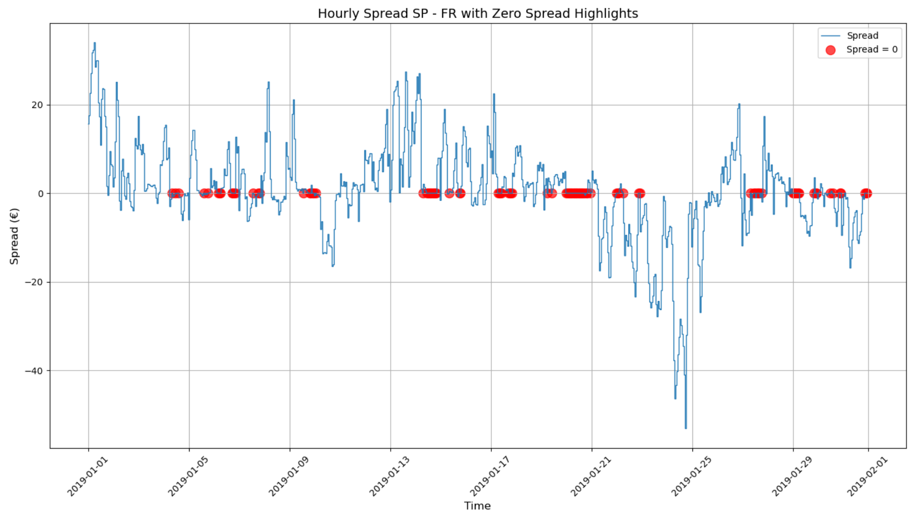

FIGURE 18: Hourly spread zero during January 2019

Note: This figure illustrates the hours during which the hourly spread for the interconnection from France to Spain was zero in January 2019. Out of the 744 hours in January, the spread was zero for 96 hours, accounting for approximately 13% of the total time.

$$\text{Value of FTR option} = \frac{1}{N} \sum_{T=T_1}^{T_N} p_T$$

, where N is the number of hours in the month